DEVELOPMENT AND SELECTION OF GLASS/SISAL AND SHEEP WOOL FIBER REINFORCED HYBRID POLYMER COMPOSITES FOR VEHICLE BUMPERS

School of Mechanical and Industrial Engineering

Ethiopian Institute of Technology - Mekelle

By: Mulu Gidey Gebretsadik(Bsc)

Seb, 2025

Mekelle, Ethiopia

Development and Selection of Glass/Sisal and Sheep Wool Fiber Reinforced Hybrid Polymer Composites for Vehicle Bumpers

A thesis submitted to School of Mechanical and Industrial Engineering, Ethiopian Institute of Technology - Mekelle

In Partial Fulfillment of the Requirements for the Masters of Science Degree in Product Design and Development

Principal investigator: Mulu Gidey Gebretsadik (BSC)

Phone NO: +251941376149

Email: 205adumech@gmail.com

Advisor: Dr. Abrha Gebregergs (Ass. Professor of ------)

Email: abrhagonder@gmail.com

Seb, 2025

Mekelle, Ethiopia

THESIS ACCEPTANCE APPROVAL FORM

"This is to certify that the thesis prepared by ***Ms. Mulu Gidey Gebretsadik*** entitled ***"Development and selection of glass/sisal/ sheep wool fiber reinforced hybrid polymer composites for vehicle bumpers"*** has been accepted for the award of the Degree of Master of Science in Mechanical Engineering (Product Design and Development), in partial fulfillment of the requirements for the Master of Science in Mechanical Engineering at Mekelle University."

Members of the Examination Board

Dr. Kalayu Mekonen		24/11/2025
External Examiner	Signature	Date
Dr Alula Gebresas		24/11/2025
Internal Examiner	Signature	Date
Dr Abrha Gebregergs		24/11/2025
Supervisor	Signature	Date
Mr Tadesse Gebray		24/11/2025
Chairman	Signature	Date

Confirmation: SMD Chair

ታደሰ ገብረ ተስፋይ (MS c)
የሶሊድ መካኒክስና ዲዛይን ቻይር ሓላፊ
Tadesse Gebray Tesfay (MS.c)
Head of Solid Mechanics & Design Chair

		24/11/2025
Chair Head	Signature	Date

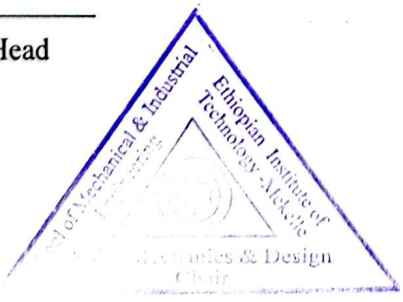

PI's DECLARATION

I affirm that this written submission reflects my own ideas expressed in my own words. For any ideas that are not my own, I have made an effort to cite and reference them appropriately. I also confirm that I have adhered to all principles of academic honesty and integrity, and I have not misrepresented or fabricated any ideas, data, facts, or sources in my submission. I understand that any violation of these principles may result in disciplinary action from the Institute and could lead to legal consequences from the sources that have not been properly cited or from whom permission has not been obtained when necessary.

Name of PI: Mulu Gidy Signature: _____ Date: _____

ADVISOR'S DECLARATION

This is to confirm that the declaration made by the candidate is accurate to the best of my knowledge, and the thesis is sufficient for the award of the degree of Master of Science in Product Design and Development.

Advisor: Dr. Abrha G/gergs (Ass. Proffesor) Signature: _____Date: _____

AKNOWLEDGMENT

First and foremost, I would like to express my gratitude to Almighty God for enabling us to be here today and for helping me overcome all the challenges to complete my thesis. I would also like to extend my heartfelt thanks to my advisor, Dr. Abrha Gebregergs, for their exceptional supervision, support, commitment, and patience throughout the entire research process. Additionally, I am grateful to the staff at the EiT-M Mechanical Engineering workshop for their guidance in facilitating the material testing during my research. I also appreciate the help and support of my colleagues who assisted me in various ways. Finally, I want to thank my family and friends for their encouragement and motivation throughout this journey.

Contents

LIST OF TABLES

LIST OF FIGURES

SYMBOLS

W_f - Weight of fiber

W_m -Weight of matrix

Wc -Weight of composite

W_{ff} -Weight fraction of fiber

W_{fm} -Weight fraction of matrix

V_f -Volume of fiber

V_m -Volume of matrix

V_c -Volume of Composite

V_{ff} -Volume fraction of fiber

V_{fm} -Volume fraction of matrix

ρ_c - Density of composite

E_1 - Longitudinal modulus of elasticity

E_2 - Transversal modulus of elasticity

E_x - In-plane longitudinal modulus

E_y - In-plane transversal modulus

G_{xy} - In-plane shear modulus

[C] - Stiffness Matrix

[Q]- Reduced stiffness

[R] - Matrix Reuter matrix

[T]- Transformation matrix

[A]- Extensional Stiffness Matrix

[B] - Coupling Stiffness Matrix

[D]- Bending Stiffness Matrix

N_x - Normal Force in x Direction

N_y - Normal Shear in y Direction

N_{xy} - Shear Force

M_x - Bending Moment in yz plane

M_y - Bending moment in xz plane

M_{xy} -Twisting moment

σ_{11L} - longitudinal tensile stress

σ_{11c} - longitudinal compression stress

σ_{22t} - Transversal Tensile Stress

σ_{22c} - Transversal Compression Stress

$V_{(X)}$ - Shear Force

$M_{(X)}$ - Bending Moment

$\delta_{(\Delta d)}$ - Deflection

K - Mid-Plane Curvatures

ε - Strain

γ - Shear Strain

υ - Poisons Ratio

τ - Shear Stress

E - Impact Energy

I - Moment of Inertia

λ - Buckling

LIST OF ABBREVIATIONS AND ACRONYMS

UD	Unidirectional
FRC	Fiber Reinforced composites
PMCs	Polymer matrix composites
CMCs	Ceramic matrix composites
MMCs	Metal Matrix Composites
PCs	Particulate Composites
SCs	Structural Composites
HDPE	High Density Polyethylene
MEKP	Methyl Ethyl Ketone Peroxide
ASTM	American society of testing materials
FMSS	Federal Motor Vehicle Safety Standards
CMVSS	Canadian Motor Vehicle Safety Standards
UDL	Uniformly Distributed Load
GSE	Ground Service Equipment
UTM	Universal Testing Machine
CLT	Classical Laminate theory
FEM	Finite Element Method
CAD	Computer Aid Design
FPF	First Ply Failure load
ROM	Rule of Mixture
Mph	Miles Per Hour
SR	Strength Ratio
Eq.	Equation
Hr.	Hour

ABSTRACT

Background: A bumper is an essential part of a vehicle, engineered to absorb impacts and shield the front and rear during low-speed collisions. This research focuses on creating glass/sisal and sheep wool fiber-reinforced composites for bumpers, meeting the demand for lightweight, sustainable materials while fostering local economic growth through job creation. It seeks to substitute traditional heavy materials, decrease costs, and advance sustainability initiatives within the automotive sector.

Objective: The primary objective of this research is to develop and select hybrid composite materials that combine glass, sisal, and wool fibers reinforced with epoxy resin for use in vehicle bumpers. Specific goals include enhancing the mechanical properties of natural fibers and optimizing the composite design for performance and cost-effectiveness.

Method: The methodology involves treating sisal and wool fibers with sodium hydroxide to enhance their mechanical properties, followed by the fabrication of composites using hand lay-up techniques. A comprehensive series of mechanical tests based on ASTM standards assesses properties such as tensile strength, impact resistance, and water absorption.

Result: The composites demonstrate a tensile strength of 114.07 MPa, impact resistance of 112.5 kJ/m², and the composite bumper can absorb a maximum energy of 49.34kJ/m^2 with speed 2.22m/s, and also a weight of 3.8 kg, significantly lighter than traditional steel bumpers (5.16 kg). Software analysis using Genetic Algorithms optimized the design, achieving a maximum stress of 31 Mpa and a deflection of 89 mm under impact conditions, indicating superior performance compared to conventional materials. This study supports the transition to environmentally friendly materials in the automotive industry.

Conclusion: This research substantiates that glass/sisal and wool fiber-reinforced composites are viable alternatives for automotive bumper applications, offering improved performance and reduced environmental impact, to reduced fuel consumption and local economic growth. The findings support the ongoing transition toward sustainable materials in the automotive industry and highlight the economic benefits associated with local fiber utilization.

Keywords: Bumper, Hybrid Glass/Sisal/Wool fiber Reinforced Composite, reinforcement, composite, tensile strength, impact resistance, optimization.

1 INTRODUCTION

1.1 Background

Vehicle bumpers are crucial components designed to absorb impact and protect a vehicle's front and rear ends during low-speed collisions. The primary purpose of bumpers extends beyond aesthetics; they are engineered to mitigate physical damage and enhance the overall safety of the vehicle. Regulations such as 49 CF R Part 581 outline the specifications and standards for these bumpers, highlighting their role in reducing damage during accidents (‘— D E C L A R A T I O N — Federal Motor Vehicle Safety , Bumper and Theft Prevention Standards’, 2022).

Bumpers consist of several parts, including the bumper cover and the reinforcement components. The bumper cover is the non-rigid outer surface that forms a significant part of the bumper's appearance and protection, while the underlying structure is typically designed to absorb energy during a collision(Rosenthal, 2009). The effectiveness of bumpers is not only a matter of design but also involves adherence to federal safety standards, ensuring that manufacturers produce vehicles capable of meeting these regulations(‘169.73 bumpers, safeguards.’, 2009).

Additionally, various jurisdictions impose specific requirements regarding bumper specifications. For example, in Minnesota, statutes mandate that all private passenger vehicles be equipped with front and rear bumpers, with some exceptions for pickups and vans. Moreover, vehicle safety standards often dictate the maximum and minimum heights for bumpers to ensure compatibility and safety among different vehicle types(No, 2023).

The material and construction of bumpers have evolved, with some manufacturers experimenting with composite materials, such as natural fibers like jute, to enhance impact strength while potentially lowering costs(Safety and Systems, 2025). This reflects a growing trend in the automotive industry that emphasizes sustainability without compromising safety. Overall, bumpers serve as a vital protective feature, reflecting a blend of safety regulations and innovative engineering in vehicle design(NHTSA, 2011).

The automotive industry is rapidly evolving, driven by the need for lightweight and cost-effective materials that enhance fuel economy and tackle pressing environmental challenges, such as global warming from high carbon emissions(Zhang and Xu, 2022). Recent research underscores the growing interest in hybrid composites, which leverage the strengths of both natural and synthetic fibers. Glass fibers offer high tensile strength and durability, while sisal fibers provide biodegradability and cost-effectiveness. Additionally, sheep wool fibers contribute unique properties like thermal insulation and sound absorption, adding value to automotive applications(Seydibeyoğlu *et al.*, 2023; Huzaifa *et al.*, 2024; Islam *et al.*, 2024).

The adoption of these composite materials not only enhances mechanical properties but also aligns with ecological and economic goals. The combination of glass, sisal, and sheep wool fibers creates a material that is both lightweight and strong, addressing critical performance parameters such as impact resistance and energy absorption. Utilizing such hybrid composites in vehicle bumpers can

lead to significant weight reductions, potentially improving fuel economy by 6-8% for every 10% decrease in weight('polymers-13-03514.pdf.crdownload', no date). Furthermore, for each kilogram of weight reduced, approximately 20 kg of carbon dioxide emissions can be avoided (Background, 2013)(Deshpande and Brown, 2022). This positions hybrid composites as an attractive solution for the automotive industry, especially since transportation accounts for 26.9% of total energy consumption in the U.S. and nearly one-third of CO2 emissions.

In conclusion, the development of glass/sisal and sheep wool fiber reinforced hybrid polymer composites for vehicle bumpers offers a promising alternative to traditional materials. By harnessing the advantages of both natural and synthetic fibers, these composites enhance vehicle safety and performance while supporting sustainability initiatives within the automotive sector. The integration of such materials can lead to significant cost savings and environmental benefits throughout the product lifecycle (Deshpande and Brown, 2022).

1.2 Problem statement

The major problems still facing the large use of composites in automotive domains are: the high cost in comparison with traditional materials (steel, alloy, aluminium), the complex and expensive manufacturing process for a large number of parts, and the unknown physical (mechanical, thermal) behaviour of some kinds of composites(Das, 2001; Belingardi *et al.*, 2015). Traditional bumper beams are made from materials such as steel and aluminum. These are heavy and can contribute to increased fuel consumption(Marzbanrad, Alijanpour and Kiasat, 2009; Belingardi *et al.*, 2015; Du *et al.*, 2023). Thus, many studies and research are conducted to solve these problems to extend the use of composites in large quantities(Das, 2001; Belingardi *et al.*, 2015). The project aims to reduce the cost, weight of composite bodies in vehicle structures for the mainstream automotive sector. Then, by utilizing hybrid composites of glass/sisal and sheep wool fibers binding with epoxy resin to achieve superior impact resistance, light-weight design, and environmental benefits, aligning with modern automotive standards.

Figure 1.1 car front and rear bumper

1.3 Scope of the study's

The scope of this study is to characterize, investigate, and design a car bumper beam from glass/sisal/sheep wool fiber reinforced polymer hybrid composites based on the collected related data and analysis. This research attains the chemical treatment of the sisal and wool natural fiber, and sample fabrication of natural and synthetic hybrid composites, characterizing the mechanical properties (tensile strength, compression strength, flexural strength, impact strength, water

absorption, and density), testing based on the ASTM standards, selecting the best stacking sequence laminate, and optimizing the glass/sisal/sheep wool fiber hybrid composite of an car bumper beam using MATLAB, and validate the optimized hybrid composite using FEM.

1.4 Significance of the study's

The significance of this study is multifaceted, addressing both environmental and economic challenges in the automotive industry. The development of hybrid glass/sisal and sheep wool fiber-reinforced polymer composites presents a sustainable alternative to traditional materials like steel and aluminum, which have higher carbon footprints and contribute to resource depletion. By utilizing natural fibers, this research not only reduces the weight of vehicle components but also enhances biodegradability, promoting a more circular economy.

Improving fuel efficiency and minimizing carbon emissions are key outcomes of this study. Lighter materials can significantly decrease fuel consumption, aligning with global initiatives aimed at mitigating climate change. This shift towards greener materials is essential for the automotive sector's sustainability efforts.

Moreover, the findings can serve as a valuable reference for future innovations in composite materials, encouraging the exploration of hybrid solutions in various applications beyond automotive. This research not only advances material science but also fosters environmental sustainability and local economic development, making it a crucial contribution to academia. Ultimately, it provides a foundation for developing hybrid composites that meet the strength requirements for automotive bumpers, while also serving as a resource for educators and researchers in the field.

1.5 Objective

1.5.1 General objective

- The main aim of this study is to develop and select hybrid composite materials (glass/sisal/wool fiber reinforced hybrid with epoxy resin) for an automotive bumper.

1.5.2 Specific objective

- To develop hybrid composites(create a combined strength of glass/sisal and wool fibers)
- To improve the mechanical properties of the sisal and wool fibers by adding the alkaline treatment of sodium hydroxide to each fiber
- To evaluate the mechanical properties of the hybrid composites(tensile strength, flexural strength, and impact resistance)
- To select more sustainable hybrid composites of glass/sisal and sheep wool fibers, binding with epoxy resin
- To design and optimize an automotive bumper using MATLAB
- To validate the design using (FEM)

2 LITERATURE REVIEW

The development and selection of glass/sisal and sheep wool fiber reinforced hybrid polymer composites for vehicle bumpers is a significant advancement in automotive materials, aimed at enhancing performance while reducing environmental impact. This literature review synthesizes findings from various studies that explore the mechanical properties, fabrication methods, and advantages of these composites over traditional materials.

2.1 Composite

Composites are heterogeneous materials having two or more solid phases, which are in intimate contact with each other on a microscopic scale. A composite consists of a matrix and reinforcement. Matrix is a medium in which the reinforcement is embedded. The matrix is of three types: ceramic, polymeric, and metallic. Reinforcement used in building the composite can be either fibrous or non-fibrous. Fibers are either derived from sources like plants or other living species, or they can be made artificially(Dugvekar and Dixit, 2021). Natural fibers such as kenaf, sisal, banana, jute, flax, hemp, curaua, and coconut are attractive alternatives to synthetic fibers for applications in the automotive and construction industries. Mechanical performance of a fiber-reinforced composite depends on the integrity of the fiber/matrix interface, which enables the strain from the matrix to the fiber. The strain transfer effectiveness plays a dominant role in determining the mechanical properties of the final product. Natural fibers have several advantages compared with synthetic fibers for reinforcement of polymer composites. They have low density, are biodegradable, abundant, non-abrasive, possess high mechanical performance, and lack toxicity(Betelie *et al.*, 2019).

A composite is a material structure composed of at least two macroscopically distinct materials that work in concert to achieve improved performance. Often referred to as fiber-reinforced plastic, composites represent a combination of various components arranged in a specific formulation. They consist of a reinforcing or filler phase and a matrix or continuous phase, which are separated by an interface phase. Typically, the discontinuous phase is stronger and harder than the continuous phase, and it is known as the reinforcement, while the continuous phase is called the matrix(Nijssen, no date)(Dugvekar and Dixit, 2021)(Bichang *et al.*, 2022)(Zoccola and Anceschi, 2024).

2.1.1 Classification of composites

Composite materials are classified into three types based on the matrix. They are Polymer matrix, Ceramic matrix, and Metal matrix composites. Polymer materials (plastics) combine fibers and matrix into a composite material(Harris, 1999). Polymers have some advantages: low density, good chemical resistance, but lack thermal stability, and have poor mechanical properties (Harris, 1999; ‘1 . Classification of Composite Materials’, 2004). Polymers are classified into two categories, depending on the processing methods. These are the thermoplastics and the thermosets. Thermosetting resins are cross-linked polymers that do not melt on heating, but ultimately disintegrate or are non-cured (Sonar *et al.*, 2015).

Composite materials are classified based on reinforcements in the form of fibers, particles, and structures. Fiber-reinforced polymer composites are load-carrying elements; the fibers can be either

synthetic fibers or natural fibers. Natural fibers like plants, animals, and minerals. The advantages of natural fibers over synthetic fibers comprise low density, low cost, availability, recyclability, and biodegradability. Whereas synthetic fibers (glass and carbon) have an advantage in high strength and high stiffness, and it has a long fatigue life and adaptability(Sonar *et al.*, 2015; Karatas, 2018).

2.1.2 Hybrid fiber-reinforced polymer composites

Hybrid composites are created using more than one reinforcing agent in a single polymer matrix to increase the composite properties(Neto *et al.*, 2022). Fiber-reinforced polymer (FRP) composite, reinforcement includes natural fibers and synthetic fibers in a polymer matrix. Natural fibers have become better replacements for synthetic fibers due to their advantages over synthetic fibers. Natural fibers show advantages such as low cost, low density, availability in abundance, environmental friendliness, nontoxicity, high flexibility, renewability, biodegradability, relative non-abrasiveness, high specific strength and modulus, and ease of processing. But natural fibers have some limitations, such as low impact strength and high moisture absorption properties. These limitations can be reduced using the hybridization technique. Hybridization can increase the mechanical properties due to the following reasons: (1) in hybridization, having two fibers with the same length and different diameters in a polymer matrix provides some advantages over the use of one fiber in the composites. The differences in the diameters of fibers increased the effective area of fiber-matrix adhesion so that uniform transfer of stress could take place. (2) The fiber having low elongation may break first, and then the load may be carried by the fiber having high elongation without the failure of the matrix, inducing better stress transfer from the matrix to fibers and thus resulting in increased mechanical properties (Ashik and Sharma, 2015; Gupta and Srivastava, 2016a; Neto *et al.*, 2022). The main factors that affect the performance of hybrid fiber-reinforced composites are the types of fiber and resin or matrix, and the effect of fiber orientation(Neto *et al.*, 2022).

2.2 Natural fibers

Natural fibers are found to be a prospective replacement for synthetic fibers in the composite sector because of their versatility and local availability. Since the dawn of civilization, natural fibers have been utilized to develop ropes, twines, fabrics, etc., and they have always played an essential role in society. Natural materials can be considered environmentally friendly as they are characterized by their renewable, biodegradable, low-density, lightweight, ease of fabrication and processing, cost-effectiveness characteristics, and low energy combustion. Wool, flax, kenaf, hemp, jute, banana, and sisal fibers are examples of natural materials that are used in industries as alternative materials regarding the manufacturing of composites (Sonar *et al.*, 2015)(Ravi, 2023)(Allafi *et al.*, 2022). Due to this, it was increasingly chosen over synthetic fibers. Moreover, fiber-reinforced composites were developed to improve the strength of weaker polymer matrix composites. Additionally, it improved not only the mechanical strength but also the material's workability. Therefore, natural fibers are frequently used as reinforcements in polymer matrices and provide a high strength-to-weight ratio(Ravi, 2023). Applications of natural fibers are found in different industries such as the civil construction industry, aerospace, and automotive industries etc(Dashtizadeh *et al.*, 2017).

2.2.1 Sisal fiber

Sisal fiber is obtained from the leaves of the plant Agave sisalana, which originated in Mexico and is now mainly cultivated in East Africa, Brazil, Haiti, India, and Indonesia(Joseph, Dias, *et al.*, 1999). The name “sisal” comes from a harbor town in Yucatan, Maya, Mexico, which means cold water. They prepared the fibers by hand and used them for ropes, carpets, and clothing. A good sisal plant yields about 200 leaves, with each sisal plant leaf containing 1000 to 1200 bundles of fibers. These bundles consist of 4% fibers, 8% dry matter, 0.75% cuticle, and around 88% water. The fibers are extracted by retting and scraping or by mechanical extraction, and the diameter of the fiber varies from 100µm to 300µm(Joseph, James, *et al.*, 1999). Once the fibers are extracted, they are washed with clean water to remove the leaf juices, adhesive solids, chlorophyll, and so on (Joseph, Dias, *et al.*, 1999; Alajmi *et al.*, 2024).

Figure 2.1 Sisal plant

2.2.2 Sheep wool fiber

Sheep wool is a byproduct of sheep farming. Wool fibers are inexpensive, biodegradable, fire-resistant, and have excellent insulating properties(Zoccola and Anceschi, 2024). Raw wool is one of the major export commodities of several countries, including Australia. It is one of the oldest naturally renewable fibers in use. It is epidermal in origin and grows naturally on the bodies of sheep. Wool is composed of a single protein called keratin, which contains the main five elements (in %): hydrogen 6–7, carbon 50, oxygen 21–24, nitrogen 15–21, sulfur 2–5, and other elements. Wool is a copolymer of 18 amino acids, whereas synthetic fibers are copolymers with two monomers. The different content of amino acids in wool fiber contributes to its advantages in chemical characterization. Cystine-containing sulfur is an important wool fiber property. Higher sulfur amount in wool means better-treating properties, higher resistance to chemical impacts, and higher physicomechanical (Allafi *et al.*, 2022). Wool fiber layers are composed of two types of cells: the internal cells of the cortex and external cuticle cells that form a sheath around the fiber.

Wool fibers variety of applications, for instance, wool fibers are used to produce lightweight and durable sports equipment or to create eco-friendly packaging materials, and are also employed in furniture production, particularly in the fabrication of chairs and tabletops. Additionally, they are utilized in the biomedical field for the production of orthopedic implants. Finally, wool fiber composites are utilized in the aerospace industry, particularly in aircraft interiors and structural components(Zoccola and Anceschi, 2024). The wool is obtained by shearing the fleece from the sheep, and graded, washed, and searched to remove any extraneous matter such as grease, dirt, moisture, and vegetable matter after all then spin.

Figure 2.2 Sheep wool

2.2.3 Synthetic fiber

Synthetic fiber is a fiber-reinforced polymer composite, which is called an artificial or man-made composite. Products of petroleum are the main source of synthetic fibers. Synthetic fibers have better properties than natural fibers. Different chemicals, having their own properties, are mainly used to produce synthetic fibers. Nylon, acrylics, polyesters, polyurethanes, etc., are synthetic fibers produced from chemical products(Gangil *et al.*, 2020). There are various types of synthetic fibers, mainly three types of synthetic fibers are used in the composite industry on a large scale: Kevlar (aramid), glass fiber, and carbon have been frequently used in aerospace and automobile industries due to low density, high stiffness, and strength. Despite these properties of synthetic fiber, they have serious drawbacks like biodegradability, recyclability, initial processing cost, and health hazards, etc(Gupta and Srivastava, 2016a).

2.2.3.1 Glass fiber

Glass fiber-reinforced polymer is made of a plastic matrix reinforced by fine fibers of glass. Glass fiber is a type of reinforcement used in polymer composites, which are made of extremely fine fibers of glass. The glass fibers can be used in many ways. They can either be woven into simple fabric, flattened, or even randomly arranged, all of which further alter the mechanical properties of the composite synthesized(Dugvekar and Dixit, 2021). Fiberglass is a lightweight, strong, and robust material used in different industries due to its excellent properties(Ashik and Sharma, 2015). GFs are also called load-bearing elements in the composite structure. GFs are most widely used among all synthetic fibers as they offer excellent strength and durability, thermal stability, resistance to impact, chemical, friction, and wear properties. However, the main drawbacks of using these fibers are their biodegradability, initial processing costs, recyclability, energy consumption, machine abrasion, health hazards, etc (Neto *et al.*, 2022).

2.2.4 Polymer matrix

The primary phase, having a continuous character, is called a matrix. Matrix is usually more ductile and less hard phase(Allafi *et al.*, 2022). In FRP composite, the matrix may be either a thermoset or a thermoplastic. Thermosets are those that cannot be heated and softened. A matrix is used to keep the fibers straight and transfer the load to the fibers. Matrix also provides rigidity and shape, and protects the fibers from chemical and corrosion effects. Thermoset polymers go one better than thermoplastics in mechanical properties, thermal stability, chemical resistance, and durability(Gupta

and Srivastava, 2016b). Polymer matrices are also divided into natural matrices and synthetic matrices, which are petrochemical-based and include polyester, polypropylene (PP), polyethylene (PE), and epoxy.

2.2.4.1 Epoxy resin

Epoxy resin is a type of thermoset polymer matrix which are widely used as a matrix material or as a binding agent in fiber-reinforced composites, primarily because of the ease of processing due to its low viscosity. The epoxy resin is the most used polymer matrix due to its high tensile strength and modulus, and high compressive strength(Rajak *et al.*, no date). Epoxy resins are relatively low molecular weight pre-polymers capable of being processed under a variety of conditions. The following are the most outstanding characteristics of epoxy for which it is used.

- Low volatility during cure.
- High gloss, crystal clear
- Excellent adhesion to different materials.
- Great strength and toughness resistance.
- Ultraviolet resistant.
- Excellent electrical insulating properties.
- Scratch-resistant.

2.3 Effect of weight on Vehicles

Composite materials that combine multiple components are increasingly utilized in the automotive industry due to their high specific strength, design flexibility, and corrosion resistance, enabling weight reductions of 15% to 40%. Glass fiber-reinforced polymer (GFRP) composites are particularly appealing for their lightweight and high performance, significantly improving fuel economy—by about 7% for every 10% reduction in weight—while enhancing energy absorption and impact resistance. Optimizing energy absorption performance is crucial for crashworthiness, with mechanisms that promote progressive failure and reduce peak loads enhancing occupant safety. Additionally, design features like foam filling and conical structures can improve energy absorption efficiency, further contributing to the structural integrity of vehicles during impact events(Mohammadi *et al.*, 2023)(Capretti *et al.*, 2024).

A glass fiber-reinforced composite bumper was designed and tested, demonstrating impressive mechanical properties: a flexural strength exceeding 0.5 kN, tensile strength of 3852.8 kJ (3.9 MJ), and impact strength of 100 kJ/m², while achieving a 60% weight reduction compared to steel bumpers. These results indicate that this composite can effectively replace steel for safer, lightweight, and corrosion-resistant automotive applications(Achema *et al.*, 2017). Additionally, a Toyota Corolla bumper made from sisal-reinforced polyester via hand lay-up showed a tensile strength of 76.47 MPa, impact strength of 32.215 kJ/m², and flexural strength of 63.66 MPa, all meeting Federal Motor Vehicle Safety Standards. Notably, the sisal composite bumper resulted in a 45.3% cost savings compared to traditional steel and plastic bumpers(Buba, Bello and Jatau, 2023).

2.4 Study on the Structural Analysis of Laminate Composite

Composite laminates, or laminated composites, consist of various plies, each treated as a unidirectional (UD) fiber lamina. The mechanical behavior of each lamina is classified as transverse isotropic, while the overall laminated composite behaves orthotropically. This construction is among the most commonly used in composites, featuring architectures like cross-ply ([0, 90]), bi-directional ([−θ, +θ]), and tri-axial laminates ([−θ, 0, +θ]). Laminated composites exhibit excellent in-plane mechanical properties, including high Young's moduli, shear modulus, and ultimate strength. However, they typically lack stiffness in the out-of-plane direction (Z direction), necessitating additional layers to enhance this property, which can increase weight and manufacturing costs, limiting complex shape production(Hochard *et al.*, 2017). Additionally, laminated composites are susceptible to delamination and interlaminar shear. These materials are widely employed across various industries, including aerospace, automotive, medical, and sports, due to their lightweight, stiffness, and customizable properties, enabling the creation of high-performance structures that often outperform homogeneous materials(Kumar, 2017).

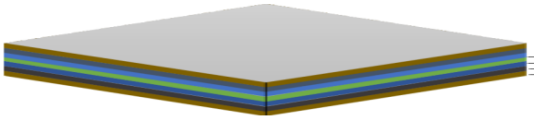

Figure 2.3 Laminates

2.5 Chemical Treatment of Natural Fiber Composite Material

Chemical treatments of natural fiber composite materials significantly improve their mechanical properties, durability, and moisture resistance. Techniques such as alkali, silane, and acetyl modifications optimize fiber-matrix adhesion and reduce hydrophilicity, which is vital for the performance of natural fiber-reinforced composites (NFPC) in various applications. Alkali treatment, typically using sodium hydroxide (NaOH), removes lignin and hemicellulose, enhancing fiber-matrix bonding(Ramasamy *et al.*, 2023). Silane treatment boosts interfacial adhesion and minimizes moisture absorption, while acetylation improves dimensional stability and reduces water uptake(Thirumalaisamy *et al.*, 2023).

These chemical treatments lead to notable enhancements in tensile strength, impact resistance, and thermal stability. For example, fibers treated with magnesium carbonate (MgCO3) show improved mechanical properties suitable for biocomposite applications. Treated natural fibers are increasingly favored in sectors like automotive and construction due to their eco-friendliness and superior performance compared to synthetic alternatives. However, the treatment process requires careful balancing of sodium hydroxide concentration and immersion time, as excessive NaOH can damage fiber particles and diminish tensile strength, while insufficient treatment may leave boundary layers intact, leading to reduced strength(Gurmu, 2023) (Ramasamy *et al.*, 2023).

2.6 Study on the mechanical properties of polymer composites

Mechanical properties of composites, such as tensile strength, flexural strength, impact strength, and hardness, were also found in hybrid composites, and chemical and flame resistance improved after the chemical treatment(Dashtizadeh *et al.*, 2017).

2.6.1 Study on Mechanical Properties of Natural/ Natural Fiber Hybrid Composites

Betelie et al. examined the effects of fiber concentration and orientation on the mechanical properties of sisal-epoxy composite plates using hand lay-up techniques. They found that alkali treatment with 10% NaOH enhanced the adhesion of sisal fibers, resulting in optimal mechanical properties at 30 wt% fiber content in symmetric orientation, yielding tensile strength and modulus values of 85.5 MPa and 4.5 GPa, respectively. In contrast, randomly oriented fibers achieved lower values of 58 MPa and 2.53 GPa. Similarly, another study on sisal fiber-reinforced polyester composites revealed that alkali treatment reduced water absorption and improved impact properties, although compressive strength declined at higher fiber contents. A. S. Blicblau et al. developed composites using raw wool and polyester resin, requiring over 50% wool by weight to achieve a six-fold increase in impact toughness compared to virgin polyester. Flexural performance was maintained at low reinforcement levels, indicating that high wool fiber volumes can effectively enhance polyester matrices. Additionally, J. Tusnim et al. explored jute and sheep wool fiber-reinforced hybrid polypropylene composites, finding that mechanical properties improved with increased fiber loading, achieving the best results at 15% fiber content with a 3:1 jute to wool ratio, paving the way for further investigations into the properties of raw versus treated fibers(Betelie *et al.*, 2019)(Melkamu, Kahsay and Tesfay, 2018)(Blicblau, 2014)(Series and Science, no date).

2.6.2 Study on Mechanical Properties of Natural/ Synthetic Fiber Hybrid Composites

Hybrid composites combine the strengths of natural fibers, like sisal, with synthetic fibers, such as glass, to create materials that are both strong and environmentally friendly. These composites exhibit enhanced mechanical properties, including tensile and flexural strength, which are significantly influenced by fiber orientation. For instance, sisal/glass composites show higher tensile strength and flexural strength in longitudinal orientations compared to transverse ones(Dashtizadeh *et al.*, 2017) (Alajmi *et al.*, 2024)(Gurmu, 2023)(Gupta and Deep, 2017).

Bichang et al. noted that chemical pretreatment with 5% NaOH improved tensile and flexural strengths of glass/sisal composites. Gupta et al. found that increasing sisal and glass fiber content in epoxy composites up to 30 wt.% enhanced tensile strength to 87.22 MPa and flexural strength to 411.43 MPa, although higher fiber content led to decreased adhesion and mechanical performance. Ali et al. compared laminated composites of glass and wool fibers, revealing significant differences in ultimate strength due to the superior tensile strength of glass fibers(Bichang *et al.*, 2022)(Gupta *et al.*, 2015)(Ali *et al.*, no date).

Ravikumar et al. reported that jute fiber reinforced polyester composites had lower mechanical properties and higher water absorption, while jute/carbon fiber hybrids showed improved

performance metrics, including tensile strength of 136.3 MPa and flexural strength of 175.8 MPa. Additionally, Arthanarieswaran et al. highlighted that hybrid banana/sisal/glass composites achieved the highest tensile strength with optimal configurations, demonstrating the potential for tailored performance in automotive applications through careful fiber arrangement and treatment(Ravikumar *et al.*, 2022)(Arthanarieswaran, Kumaravel and Kathirselvam, 2014).

2.7 Composite manufacturing techniques

Composite materials can be fabricated using various techniques, which are essential to achieving specific material properties and production requirements. The selection of fabrication methods depends on several factors, including production volume and rate, economic considerations, availability of materials, required skills, surface complexity, and the size of the product. Each application field may require different fabrication procedures tailored to these parameters(Presentation, no date; Sticklen *et al.*, 1992). In the manufacturing of fiber-reinforced thermoset composites, there are several key fabrication techniques available, such as Hand lay-up, Compression molding, Resin transfer molding (RTM), and Injection molding. Hand lay-up technique involves manually placing layers of reinforcement into a mold, which is suitable for low-volume production. Compression molding and RTM are more suited for higher-volume applications, as they offer faster production rates and more consistent quality. Injection molding has the advantage of allowing for complex shapes and high precision in the final product(Sticklen *et al.*, 1992; Kumar and Shelare, 2019).

Each fabrication technique offers distinct advantages and is selected according to the specific needs of the project at hand, balancing factors like labor intensity, tooling requirements, and equipment availability to achieve optimal results in composite manufacturing. Selecting an appropriate fabrication method ensures that the composites meet the desired specifications while maintaining economic viability(Nagavally, 2016; Pellicer, 2021).

2.7.1 Hand lay-up technique

Hand lay-up is one of the oldest open mold composite processing methods. It is a composite laminating process in which layers of resin and reinforcement are applied manually on top of an open mold surface one by one until the desired thickness of the component is obtained. There are five main steps in the hand lay-up process: cleaning, gel coating, laying-up, curing, and part removal(Nagavally, 2016). In hand lay-up techniques, there are four essential procedures, and a typical schematic diagram for hand lay-up technique is Mold preparation, Demold coating, Lay-up, and Resin pouring and smearing shown in the Figure below.

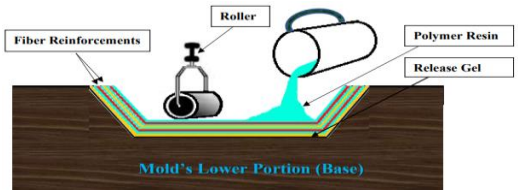

Figure 2.4 Hand lay-up

2.8 Optimization with Genetic Algorithm

Genetic algorithms are a type of optimization algorithm, meaning they are used to find the optimal solution(s) to a given computational problem that maximizes or minimizes a particular function. Genetic algorithms are iterated until the fitness value of the best-so-far chromosome(variable) stabilizes and does not change for many generations. This means the algorithm has converged to a solution(s)(Carr, 2014).

Genetic algorithms are adaptive heuristic search algorithms premised on Darwin's evolutionary ideas of natural selection and genetics. The basic concept of genetic algorithms is designed to simulate processes in natural systems necessary for evolution. A population of individuals is maintained within the search space for a GA, each representing a possible solution to a given problem. Each individual is coded as a finite-length vector of components, or variables, in terms of some alphabet, usually the binary alphabet {0, 1}. To continue the genetic analogy, these individuals are likened to solutions and the variables(Bajpai, no date).

3 METHOD AND MATERIALS

This study describes the raw materials used, the manufacturing process, and the fabrication of laminates, test setup, loading protocols, and experimental results of reinforcement materials that constitute the hybrid composites. The characterization of the laminates of composite material is based on the ASTM standard. The best material laminate is selected based on impact strength and then designed and optimized using a Genetic algorithm and validated using FEM (Abaqus) analysis.

3.1 Materials

3.1.1 Fiber Reinforcements

3.1.1.1 Sisal Fiber

The sisal fiber is extracted from the leaves of the Agave species, Agave Sisalana, and it is found in southern Mexico, but it is widely available and cultivated in Asia and East Africa. Sisal fiber is widely available in Ethiopia and yields a stiff fiber used in making various products like rope, mats, carpets, handbags, etc. Sisal fiber is widely used as a reinforcement material in many different fiber-reinforced composite materials. Sisal fiber characteristics are low density, biodegradable, and cost-effective. The fiber was obtained from the local area around Mekelle city. Sisal fibers are extracted

from the sisal plant leaves by hand using a knife. The fibers were washed and separated until individual fibers were identifiable, then sun-dried the remove moisture.

Figure 3.1 sisal fiber extraction

Table 3.1 Physical, mechanical, and chemical Properties of the sisal fiber(Bichang et al., 2022)(Alajmi et al., 2024)

Physical properties	Values	Units
Density ρ	1.3-1.5	g/cm^3
Young's modulus	10-30	GPa
Shear modulus's	4-10	GPa
Elongation at break	6-7	—
Cellulose content (%)	60–65	—
Lignin content (%)	10–14	—
Tensile strength	511–635	MPa
Shear stressτ_{12}	20-30	MPa
Longitudinal Young's modulus	9–22	GPa
Transversal Young's modulus	3.85 ± 0.87	GPa
Poisson's ratio	0.2-0.3	—

3.1.1.2 Sheep Wool Fiber

Wool fiber is a natural fiber obtained from sheep by shearing the wool and has a very complex structure. This complex structure has characteristics of excellent flexibility, moisture absorption, flame resistance, warmth, coolness, odor absorption, biodegradability, recyclability, breathability, resilience, softness, absorbs noise, is safe, and easy to handle. Sheep were bought from the marketplace and sheared the sheep wool by graded, washed, and combed to remove impurities.

Table 3.2 Mechanical properties of sheep wool fiber(Allafi et al., 2022) (Zoccola and Anceschi, 2024)

Parameters	Values	Units
Density ρ	1.3-1.4	g/cm^3
Young's modulus, E_f	0.2-4	GPa
Shear modulus, G_{12}	0.5-1.5	Gpa
Poisson's ratio(v_{12f})	0.3-0.5	-
Diameter	10-30	µm
Shear stressτ_{12}	5-10	MPa

Figure 3.2 Sheep wool preparation

3.1.1.3 Glass Fiber

Glass fiber-reinforced polymer is made of a plastic matrix reinforced by fine fibers of glass. E-glass is by far the most commonly used glass. Its characteristics are Lightweight, strong, and known for high tensile strength and durability, and it is the least expensive and also a very good conductor of electricity. E-Glass fiber is one of the most commonly used synthetic fibers, manufactured with raw materials such as limestone, silica, clay, fluorspar, and dolomite(Arthanarieswaran, Kumaravel and Kathirselvam, 2014). Glass fiber is manufactured from fine strands of glass purchased from Mekelle local city roto fiber production with a cost of 500 ETB per kilogram.

Figure 3.3 Glass fiber

Table 3.3 Mechanical properties of E-glass fiber (Dugvekar and Dixit, 2021).

Parameters	Values	Units
Density ρ	2.54	g/cm^3
Longitudinal modulus, E_{1f}	85	GPa
Transversal modulus,E_{21f}	85	GPa
Axial shear modulus, G_{12f}	30	GPa
Transverse shear modulus, G_{23f}	30	GPa
Poisson's ratio(v12f)	0.25	-
Shear stress τ_{12}	60-100	MPa

3.1.2 Matrix Material

3.1.2.1 Epoxy Resin

Epoxy resin is a type of thermoset polymer that is widely used as a matrix material or as a binding agent in fiber-reinforced composites, primarily because of the ease of processing due to its low viscosity. From polyester and epoxy polymers, the epoxy polymer resin is preferable for fiber-reinforced composite manufacturing. It was mixed with the hardener iron shark epoxy in a proportion

of 3:1. Its characteristics are High tensile strength, good adhesion properties, and excellent chemical resistance. The resin has a low viscosity and is free of any residual solvent. Epoxy resin possesses aromatic groups, which makes it three times more powerful than polyvinyl resin. Moreover, it tends to withstand much greater impacts than either polyvinyl or polyester resin due to its high thermal stability. Hence, the epoxy had better mechanical properties than polyester and polyvinyl resin(Alajmi *et al.*, 2024). Epoxy resin is obtained from Mekelle local city around Jebruk for 1500 ETB per Liter.

Figure 3-4 Epoxy with hardener

Table 3.4 Properties of epoxy resin (Bichang et al., 2022)

Parameters	Values	Units
Density ρ	1.3	g/cm^3
Young's modulus, E_m	3.5	Gpa
Shear modulus, G_m	1.26	Gpa
Poisson's ratio v_{mf}	0.36	—
Tensile strength, σ_{tm}	80	MPa
compressive strength, σ_{cm}	104	MPa
Shear strength τ_{12}	30-80	MPa
Coefficient of thermal expansion, α_{1f}	62	10^{-6}/°C

3.1.3 Tools, machines, and other necessary devices

The main tools used for the project are an oven, a manual stirrer, an electronic balance, a roller, a cutter, a wooden plate, a ruler, a press load, cups, and a testing machine. The electronic balance is used for weighing resin and fibers to ensure precise measurement. Release wax is utilized in laminates to stop the bonding of the molding material with the mold. Some additional tools and necessary items for composite production include a cleaner, hammer, brush, gloves, caliper, scissors, cloth, and meter.

3.2 Methodology

3.2.1 Preparation of Fiber Reinforcements

3.2.1.1 Sisal Fiber Treatment

Chemical Treatment of Sisal fibers was performed with NaOH aqueous solution having different concentrations, i.e., 5%, 10%, 15%, and 20% for 24h at room temperature(Sosiati and Rizky, no date). Tensile strength and modulus of sisal fiber were found to be maximum above 5% alkali, and beyond it decreasing trend was found. The increase in the tensile strength and modulus of 10%

alkali-treated sisal fiber is mainly because of the removal of hemicellulose, which causes close packing of cellulose fibrils by forming strong hydrogen bonds. Raw sisal fibers are soaked in an 8% solution of caustic for 24 h and then washed several times with distilled water; the fibers are then dried in the sun for 24 h.

3.2.1.2 Wool Fiber Treatment

Chemical treatment operation was performed upon the wool fiber as follows. Firstly, wool was washed repeatedly in clean running water and then dried. After drying, the wool was submerged for three hours in a solution consisting of 2% sodium hydroxide and 98% distilled water to soften. Lastly, the fibers were taken out and then washed in running water for two hours. This treatment enhances bonding during composite formation.

Figure 3.4 Sisal and wool fiber before and after treatments

3.2.2 Molding Process

A mold is prepared to shape the composite material from wood 310x210x5 mm^3. Casting the mixture of glass/sisal/wool fibers and epoxy resin is poured into the mold and allowed to cure at room temperature or in a controlled environment.

3.2.3 Curing

The mixture is cured for a specific duration (typically 24-72 hours) to achieve full strength. Post-curing, additional heat treatment may be applied to enhance the mechanical properties of the cured composite.

3.2.4 Rule of mixture (ROM) of a composite based on mass & Volume Ratio

In the design, fabrication, and analysis of composite materials, determining the percentages of ingredients, such as the fiber-to-matrix fraction, is essential. This is necessary to prepare and estimate the size of the composite laminate, enhance the mechanical properties of the laminate by adjusting these values, and minimize waste of composite constituents. So, Properties that obey the rule of Mixture can be calculated as the sum of the value of the property of each constituent of the hybrid multiplied by its respective weight or volume fraction in the mixture.

$$PI = P_1 V_1 + P_2 V_2 \quad \text{3.1}$$

when, PI = property of Composite to be investigated,

P_1 & P_2 = properties of the first and second systems, respectively

V_1 & V_2 = Volume Fraction of first and second system, respectively. Therefore, to go through the rule-of-mixtures, here are the steps to be followed.

3.2.4.1 Fiber and matrix weight and volume fraction content of the composites

i. Fiber and matrix mass fraction (M_F, M_M)

Total mass of composite = mass of fiber + mass of matrix

$$W_C = W_F + W_M \quad \text{..... 3.2}$$

Fiber mass fraction $\frac{\text{weight of fiber}}{\text{total weight}}$

$$W_{fF} = \frac{W_F}{W_F + W_M} \quad \text{..... 3.3}$$

Matrix mass fraction $\frac{\text{mass of matrix}}{\text{total mass}}$

$$W_{fM} = \frac{W_M}{W_F + W_M} \quad \text{..... 3.4}$$

And; $M_F + M_M = 1$

ii. Fiber and matrix volume fraction (V_F, V_M)

$$V_C = V_F + V_M \quad \text{..... 3.5}$$

The volume of fiber $= \frac{\text{weight of fiber}}{\text{density of fiber}}$

$$V_{fF} = \frac{V_F}{V_F + V_M} = \frac{W_F \times \rho_M}{W_F \times \rho_M + W_M \times \rho_F} \quad \text{..... 3.6}$$

Matrix volume fraction $\frac{\text{weight of matrix}}{\text{density of matrix}}$

$$V_{fM} = \frac{V_M}{V_F + V_M} = \frac{W_M \times \rho_F}{W \times \rho_M + W_M \times \rho_F} \quad \text{..... 3.7}$$

And; $V_F + V_M = 1$

Table 3.5 Weight and weight fraction of fibers (Glass, sisal, and wool fiber) and matrix

No. laminates	weight of fiber(g)			weight fraction of fiber(%)			weight of matrix (g)	weight of composite (g)	weight fraction of matrix(%)
	G	S	W	G	S	W	E	W_C	E
GSWSG	47.8	23.2	8.1	8.25	4	1.4	500	579.1	86.35
SGWGS	47.8	23.2	8.1	8.25	4	1.4	500	579.1	86.35
WWWWW	-	-	40.1	-	-	7.5	500	540.1	92.5
SSSSS	-	69.6	-	-	12.2	-	500	569.6	87.8
GGGGG	143.4	-	-	22.3	-	-	500	643.4	77.7

Table 3.6 Volume and volume fraction of fiber and matrix

No. Laminates	Volume of fiber (cm^3)			Volume of matrix (cm^3)	Volume fraction of fiber(%)			Total volume fraction of fiber and matrix (%)		Total Volume of composite (cm^3)
	G	S	W	E	G	S	W	V_{FF}	V_{FM}	V_C
GSWSG	18.8	16.4	6.23	384.6	18	18	9	45	55	426.03

SGWGS	18.8	16.4	6.23	384.6	18	18	9	45	55	426.03
WWWWW	-	-	6.23	384.6	-	-	45	45	55	390.83
SSSSS	-	16.4	-	384.6	-	45	-	45	55	401
GGGGG	18.8	-	-	384.6	45	-	-	45	55	403.4

iii. Theoretical Density of the composite

If the fibers and Matrix are Synthetic, their density can be obtained from the manufacturer. But if they are natural, their actual density can be determined experimentally or taken from previous literature. The density of epoxy, glass, sisal, and wool fibers was found from some literature. Then, the theoretical density of the composite in terms of mass fraction can easily be obtained using the following equations.

$$\rho_C = \frac{W_C}{V_C} = \frac{W_F + W_M}{W_F \times \rho_M + W_M \times \rho_F} \quad \text{..... 3.8}$$

Table 3.7 Theoretical and actual density of composites

Sample	Theoretical density=Wc/Vc(g/cm^3)	Actual density or measured(g/cm^3)
GSWSG	1.359	1.348
SGWGS	1.359	1.33
WWWWW	1.382	1.26
SSSSS	1.42	1.18
GGGGG	1.595	1.41

3.2.5 Composite Fabrication

Preparations of a hybrid composite

The composite materials were prepared by using the hand layup method. It includes the design of fiber orientation, ply arrangement, and casting of prepared composite materials. In the hand lay-up technique, the fibers were arranged in the mold by hand, and the epoxy mixture (3:1) was poured for every layer. After that, it was compacted with a lightweight press. For the second layer of the reinforcement, the fibers were placed on the resin surface and then rolled to remove the entrapped air and to uniformly spread the mixture. The process is repeated for all plies of the reinforcement and resin until the desired thick composite. The compression process was done by using a load of around 200N for 24 hours. Then, the composite material and placed outside to dry at room temperature for 24-48hours. In this study, fibers were oriented in the mat orientations, equal to the length of the mold i.e. ~ 300 mm, and the sisal-glass and wool fiber-reinforced epoxy composite samples were prepared with weight fractions of fiber-matrix 45/55 for all batches of stacking sequences (GSWSG, SGWGS, WWWWW, SSSSS, GGGGG) of composite materials.

Specimen Preparation

pecimen is a small piece with its Appropriate dimension taken from the sample produced for the test to know mechanical properties like Tensile test, Compression test, Flexural test, Impact test, and Water absorption test according to ASTM, and taking two per each weight ratio to estimate the average value.

Figure 3.5 Prepared composite samples

3.3 Testing and Evaluation

3.3.1 Mechanical Testing

The testing machines are universal tensile testing equipment/Microcomputer Controlled Electro-Hydraulic Servo Universal Testing Machine, Model: SI-1000KN (for tensile & compressive strength, flexural strength), and charpy impact testing machine/Pendulum Impact Testing Machine, Model: SI-42, Impact Energy 150 J (for impact strength).

3.3.1.1 Tensile Strength

The strength of the composite under tension was evaluated using a universal testing machine according to ASTM D3039-2017 standards(Method, 2002). This tensile testing measures the longitudinal force needed to fracture a polymer composite specimen and the extent of its elongation at the breaking point. The standard specimen size for this test features a rectangular cross-section measuring 250 mm in length, 25 mm in width, and 3 mm in thickness. During the test, specimens were secured in the grips of the universal testing machine at a specified grip separation and pulled until failure at a rate of 5 mm/min, as per the machine specifications. The results were then recorded on a computer connected to the machine in the Civil Engineering Department on campus

Figure 3.6 Tensile test using a universal machine

The tensile strength, percentage elongation, and tensile modulus of the composite material were calculated using the equations below.

$$\text{Tensile strength} = \frac{\text{load at break (maximum load)}}{\text{width} \times \text{thickness}}$$

$$\%\ \text{elongation} = \frac{\text{elongation at rupture}}{\text{initial gauge length}}$$

The slope of the curve defines the Modulus of Elasticity. The modulus of elasticity (Young's Modulus) is the ratio of stress in MPa to strain in millimeters per millimeter (mm/mm).

$$\text{Modulus (Mpa)} = \frac{\Delta\text{Stress(Mpa)}}{\Delta\text{Strain(mm/mm)}}$$ To find the modulus by taking any two points on the modulus line, & dividing the differential between their stress values in MPa by the strain differential in mm/mm.

3.3.1.2 Compressive strength

According to ASTM D 3410M (Method, no date) Compression strength test experiment involved subjecting the specimen to axial compression loading using the UTM. The dimensional size of the specimen is (150x25x3) mm. The samples were then placed between the compression anvils to commence compression testing. During testing, the maximum load attained was recorded by the UTM testing system after the specimen failed. Laminate Compressive Strength (σ_c) is calculated using the following equation.

$$\sigma_C = \frac{F_c}{A} = \frac{F_C}{t \times w} \quad \text{.....Equation 3.9}$$

Figure 3.6 Compression test using a universal machine

3.3.1.3 Flexural Strength

The composite's resistance to deformation was evaluated through three-point bending tests, following ASTM D7249(D790) standards(Specimens and Materi-, 2010). This flexural test measures the force required to bend a composite using a rectangular cross-section bar supported on a beam, with 3-point loading applied. The standard specimen dimensions are 4 mm in thickness, 20 mm in width, and a length that is 20% longer than the support span, typically measuring 150 mm x 12.7 mm x 3 mm. If the standard specimen is unavailable, alternative sizes may be utilized. The test procedure involves arranging two bending beams for the three-point loading system, placing the specimen on the support span, and applying the load to the center with a loading nose until failure occurs at a specified rate. The resulting data is displayed on a connected computer. The flexural stress during the test is calculated using a specific formula.

$$\sigma = \frac{3PL}{2bt^2} \quad \text{..... 3.10}$$

When: σ = stress,p = Applied Force and t = thickness

- The flexural chord modulus of elasticity is the ratio (slope) of stress range and corresponding strain Range and is calculated using the following formula

$$E_f = \frac{\Delta\sigma}{\Delta\varepsilon} \quad \text{..... 3.11}$$

Where: E_f = flexural chord modulus of elasticity (MPa)

$\Delta\sigma$ =difference in flexural stress between the two selected strain points (MPa)

$\Delta\varepsilon$ = difference between the two selected strain points

- The data documented from the 3-point bend test above can be used to determine the interlaminar shear strength (SS) using the Equation below,

$$SS = \frac{3P}{4bt} \quad \text{.....3.12}$$

Figure 3.7 Flexural test using a universal machine

3.3.1.4 Impact Resistance

Measured using Charpy or Izod tests (D6110 or ISO 179-1) to evaluate the durability under sudden forces. Impact test is the impact resistance of a material, which measures the amount of force needed to break a specimen under a high-speed load introduced through a swinging pendulum.

A. A Specimen Size: The Charpy impact test was carried out for the sample's specimens with dimensions of 80mm x 10 mm x 4mm as shown in Figure 3-9 below.
B. Test Procedure After fixing of specimen pendulum is released and allowed to strike until failure occurs. The machine pendulum energy engaged for the testing was 2 Joules with a speed of 2 m/s & having a 25-kg weight mounted in the material testing laboratory on our campus. Finally, the Impact energy measured in joules was recorded from the apparatus.

Figure 3.8 Impact test using a Charpy impact machine

Impact strength = $\frac{E}{A}$, Where E is energy which reads from the machine

3.3.2 Physical testing

3.3.2.1 Water absorption test

According to ASTM D5225(ISO62)(ISO, 2008), Water absorption characteristic is another important and mandatory property for natural fiber composites since they are applied in automotive, aerospace, and marine applications. Moisture Absorption of Composites is a gravimetric test method that change in moisture content by measuring the total mass over time when exposed to a specified environment.

A. Specimen size: The specimen has a dimension of (60 x 60 x 4) mm^3 shown in Figure 3-10
B. Test Procedure: First of all, the specimens must have dried in the sun for at least 2days and then allowed to cool until they reach room temperature. The dried spacemen were weighed before and after immersion using a balance electro mass testing machine having a precision of 0.0001 (g). This procedure is repeated until there is no discernible increase in specimen weight for each sample containing different weight fractions.

C. Immersion Time: It is a time recorded at which the composite's specimen is soaked deeply into distilled water, which can be 72 hrs. The specimen removed from the water must be wiped off with a dry cloth and weighed.

$$\%\ water\ absorption = \frac{W_f - W_i}{W_i} \times 100 \quad \text{..... 3.13}$$

When: W_i is the initial weight and W_f is the final weight of the sample after immersion

3.3.2.2 Density

Determination of density according to Archimedes' principle. The density of the composite laminate sample can be determined experimentally using Archimedes' method with distilled water whose specific mass is known (0.998 g/cm^3). The dimension of the sample is 60 x 20 mm^2. The apparatus used to determine the density of the Laminated composite is:

A. Analytical Balance: to measure the sample's weights with having precision of 0.0001g.
B. Sample Holder: a wire to hold the sample when immersing it in the water
C. Immersion Vessel: A beaker for holding the water and the immersed specimen.
D. Thermometer: A thermometer used to measure the water temperature.

1. Test Procedure: According to Archimedes' principle, when an object is immersed in a liquid, the apparent loss in its weight is equal to the up thrust, and this is equal to the weight of the liquid displaced. Steps to calculate the arithmetic average of the density are.
   1. First, dry the specimens in the oven and measure them in air to find their mass in Kg.
   2. Measure and record the water temperature.
   3. Suspend the specimen using a wire about 20-30 mm above the vessel support.
   4. Determine the mass of the suspended specimen to the required precision. Record this apparent mass as the mass of the specimen and the partially immersed wire in liquid.
   5. Weigh the sample holder in water with immersion to the same depth as used in the previous step.

Then the actual (measured) density of the composite is obtained using equation 3-14 below.

$$\rho_a = \frac{\rho_w W_a}{W_a - W_w - W_h} \quad \text{..... 3.14}$$

When ρ_a is the actual density of the composite, ρ_w is the density of distilled water, W_a is the weight of the sample in air, W_w is the weight of the sample in water, and W_h is the weight of the sample holder wire in water. Again, the theoretical density of composite materials (ρ_t) in terms of weight fraction can easily be obtained using the following equation 3-15 below.

$$\rho_t = \frac{1}{\frac{W_G}{\rho_G} + \frac{W_S}{\rho_S} + \frac{W_W}{\rho_W} + \frac{W_M}{\rho_M}} \quad \text{..... 3.15}$$

where W_G, W_S, W_W, and W_m are weight ratios and ρ_G, ρ_S, ρ_W, and ρ_M are densities of Glass, Sisal, Wool, and epoxy resin, respectively. Void content of a composite may significantly affect its mechanical properties & quality of composites. i.e., higher void contents usually mean lower fatigue resistance, greater susceptibility to water penetration and weathering, and increased variation in strength properties. The presence of voids will add to the total volume, but not to the weight of the composite. According to ASTM D2734 void percentage of the composite is given by

$$Vc = 100\left(\frac{\rho_t - \rho_a}{\rho_t}\right) \quad \text{.....3.16}$$

3.4 Macro Mechanic-Laminate Design (CLT)

The classical lamination theory (CLT) is utilized to determine the stresses and strains at any position of laminates subjected to force and/or moment resultants. Assumptions used in classical lamination theory are

- Each lamina is homogeneous and orthotropically bonded together
- Displacements < thickness(t) and (t) is much < than lengths of the plate
- Transverse and shear strains (γxz and γyz) are negligible
- The transverse normal strain (εz) is negligible

And its limitationes are used in CLT

- In accurate for thicklaminates
- Can not predict interlaminar stress
- No damage or failure prediction
- Use linear only

3.4.1 Hooke's Law for a 2D Orthotropic Unidirectional & Angle Lamina

1. For Orthotropic (Orthogonally Anisotropic)

An orthotropic material is when a material has three mutually perpendicular planes of material symmetry arranged in a rectangular array, and whose stiffness matrix is given by

$$\{\sigma\} = [Q]\ \{\varepsilon\}$$

$$\begin{Bmatrix} \sigma_{11} \\ \sigma_{22} \\ \sigma_{33} \\ \tau_{23} \\ \tau_{13} \\ \tau_{12} \end{Bmatrix} = \begin{bmatrix} Q_{11} & Q_{12} & Q_{13} & 0 & 0 & 0 \\ Q_{21} & Q_{22} & Q_{23} & 0 & 0 & 0 \\ Q_{31} & Q_{32} & Q_{33} & 0 & 0 & 0 \\ 0 & 0 & 0 & Q_{44} & 0 & 0 \\ 0 & 0 & 0 & 0 & Q_{55} & 0 \\ 0 & 0 & 0 & 0 & 0 & Q_{66} \end{bmatrix} \begin{Bmatrix} \varepsilon_{11} \\ \varepsilon_{22} \\ \varepsilon_{33} \\ \gamma_{23} \\ \gamma_{13} \\ \gamma_{12} \end{Bmatrix} \quad \text{..... 3.17}$$

2. For Unidirectional along the 1–2 coordinate system

A unidirectional lamina falls under the orthotropic material category. If the lamina is thin and does not carry any out-of-plane loads, it can be assumed as plane stress conditions for the lamina.

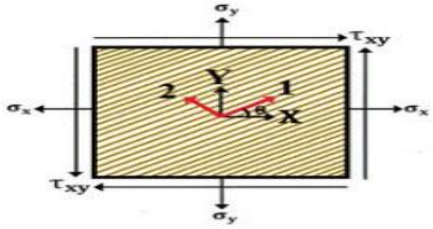

Figure 3.9 Local and global axes of an angle lamina

Therefore, taking the above Equations (3.17) and

Assuming, $\sigma_{33} = 0$, $\tau_{23} = 0$, $\tau_{13} = 0$, and $\varepsilon_{33}=0$, $\gamma_{23} = \gamma_{31} = 0$, then Hooke's law reduces to the following equation of stress–strain relationship stiffness matrix in the 1–2 coordinate system

$$\begin{Bmatrix}\sigma_{11}\\ \sigma_{22}\\ \tau_{12}\end{Bmatrix}=\begin{bmatrix}Q_{11} & Q_{12} & 0\\ Q_{12} & Q_{22} & 0\\ 0 & 0 & Q_{66}\end{bmatrix}\begin{Bmatrix}\varepsilon_{11}\\ \varepsilon_{22}\\ \gamma_{12}\end{Bmatrix} \quad \text{3.18}$$

Where: Qij are the reduced stiffness coefficients and whose values are given as follows

$$Q_{11}=\frac{E_1}{1-V_{12}\times V_{21}} \quad \text{3.19}$$

$$Q_{12}=\frac{V_{12}\times E_2}{1-V_{12}\times V_{21}} \quad \text{3.20}$$

$$Q_{22}=\frac{E_2}{1-V_{12}\times V_{21}} \quad \text{3.21}$$

$$Q_{66}=G_{12} \quad \text{3.22}$$

When E_1, E_2 are the modulus of elasticity in the fiber (1), transverse (2) direction, respectively,
-ν is Poisson's ratio, τ is shear stress,

- G is the shear modulus, which is a function of the two elastic constants $G=\frac{E}{2(1+\nu)}$ and $\tau=\frac{G}{2\pi}$ Again, the Poisson's ratio of the laminate is the ratio of $\frac{\text{Lateral(3-4 times< axial)}}{\text{Axial}}$ which is the slope obtained by plotting lateral strain against axial strain. But since the Straino meter of the universal testing machine is not working, it is calculated in the fiber direction using ROM ($V=V_{fF}V_F+V_{fM}V_M$) (Harris, 1999). By inverting the above Equation (3.18) to get the compliance matrix as

$$\begin{Bmatrix}\varepsilon_{11}\\ \varepsilon_{22}\\ \gamma_{12}\end{Bmatrix}=\begin{bmatrix}\frac{1}{E_{11}} & -\frac{V_{12}}{E_{11}} & 0\\ -\frac{V_{12}}{E_{11}} & \frac{1}{E_{22}} & 0\\ 0 & 0 & \frac{1}{G_{12}}\end{bmatrix}\begin{Bmatrix}\sigma_{11}\\ \sigma_{22}\\ \tau_{12}\end{Bmatrix} \quad \text{3.23}$$

3. For Angled Unidirectional along–y coordinate system

Generally, a laminate does not consist only of unidirectional laminae because of their low stiffness and strength properties in the transverse direction. Therefore, some laminae are placed at an angle. The coordinate system is shown in Figure 3.10. along 1–2 is called the local axis (material axis) whose direction -1 is parallel to the fibers called the longitudinal direction L, and direction -2 is perpendicular to the fibers, called the transverse direction T. The axis in the x–y coordinate system is called the global axis or the off-axis. The angle between the two axes is denoted by an angle θ. The global and local stresses in an angle lamina are related to each other through the angle of the lamina θ as follows.

$$\begin{Bmatrix}\sigma_X\\ \sigma_Y\\ \tau_{XY}\end{Bmatrix}=[T]^{-1}\begin{bmatrix}\sigma_1\\ \sigma_2\\ \tau_{12}\end{bmatrix}=\begin{bmatrix}C^2 & S^2 & 2CS\\ S^2 & C^2 & -2CS\\ -SC & SC & C^2-S^2\end{bmatrix}\begin{bmatrix}Q_{11} & Q_{12} & 0\\ Q_{12} & Q_{22} & 0\\ 0 & 0 & Q_{66}\end{bmatrix}\begin{Bmatrix}\varepsilon_{11}\\ \varepsilon_{22}\\ \gamma_{12}\end{Bmatrix} \quad \text{3.24}$$

$$[T]=\begin{bmatrix}C^2 & S^2 & 2CS\\ S^2 & C^2 & -2CS\\ -SC & SC & C^2-S^2\end{bmatrix}$$

Where, transformation matrix, C= cos (θ), and S = sin (θ). The global and local strains can also be related through the transformation matrix and rewritten as

$$\begin{Bmatrix}\varepsilon_{11}\\ \varepsilon_{22}\\ \gamma_{12}\end{Bmatrix}=[R][T][R]^{-1}\begin{Bmatrix}\varepsilon_X\\ \varepsilon_Y\\ \gamma_{XY}\end{Bmatrix} where\ [R]=\begin{bmatrix}1 & 0 & 0\\ 0 & 1 & 0\\ 0 & 0 & 2\end{bmatrix} \quad \text{3.25}$$

[R] is the Reuter matrix

Then, substituting eq(3.25) in to Equation(3.24)

$$\begin{Bmatrix}\sigma_X\\ \sigma_Y\\ \tau_{XY}\end{Bmatrix} = [T]^{-1}[Q][R][T][R]^{-1}\begin{Bmatrix}\varepsilon_X\\ \varepsilon_Y\\ \gamma_{XY}\end{Bmatrix} = \begin{bmatrix}\bar{Q}_{11} & \bar{Q}_{12} & \bar{Q}_{16}\\ \bar{Q}_{12} & \bar{Q}_{22} & \bar{Q}_{26}\\ \bar{Q}_{16} & \bar{Q}_{26} & \bar{Q}_{66}\end{bmatrix}\begin{Bmatrix}\varepsilon_X\\ \varepsilon_Y\\ \gamma_{XY}\end{Bmatrix} \text{.....3.26}$$

Where $\bar{Q}ij$ are called the elements of the transformed reduced stiffness matrix and are given by

$\bar{Q_{11}} = Q_{11}\,C^4 + Q_{22}\,S^4 + 2(Q_{12} + 2Q_{66})\,S^2C^2$
$\bar{Q_{12}} = (Q_{11} + Q_{22} - 4Q_{66})\,S^2\,C^2 + Q_{12}(\,C^4 + S^2\,)$
$\bar{Q_{16}} = (Q_{11} - Q_{12} - 2Q_{66})\,C^3S - 2(Q_{22} - Q_{12} - 2Q_{66})\,S^3C$
$\bar{Q_{22}} = Q_{11}\,S^4 + Q_{22}\,C^4 + 2(Q_{12} + 2Q_{66})\,S^2\,C^2$
$\bar{Q_{26}} = (Q_{11} - Q_{12} - 2Q_{66})^3 - (Q_{22} - Q_{12} - 2Q_{66})\,C^3S$
$\bar{Q_{66}} = (Q_{11} + Q_{22} - 2Q_{12} - 2Q_{66})\,S^2\,C^2 + Q66(\,C^4 + S^2\,)$

For finding the engineering Moduli of elasticity (E_x, E_y), in-plane shear modulus of elasticity (G_{xy}), and Poisson's ratio (ν_{xy}) of an Angle Lamina.

1. Modulus of elasticity in direction "X" (E_x) when $\sigma_y = \tau_{xy} = 0$, but $\sigma_x \neq$

$$E_X = \frac{\sigma_X}{\varepsilon_X} = \frac{1}{S_{11}} = \frac{1}{\frac{1}{E_{11}}C^4 + \left[\frac{1}{G_{12}} - \frac{2V_{12}}{E_{11}}\right]S^2C^2 + \frac{1}{E_{22}}S^4} \text{..... 3.27}$$

2. Modulus of elasticity in direction "Y" (E_y) when $\sigma_x = \tau_{xy} = 0$ but $\sigma_y \neq 0$

$$E_Y = \frac{\sigma_Y}{\varepsilon_Y} = \frac{1}{S_{22}} = \frac{1}{\frac{1}{E_{11}}S^4 + \left[\frac{1}{G_{12}} - \frac{2V_{12}}{E_{11}}\right]S^2C^2 + \frac{1}{E_{22}}C^4} \text{..... 3.28}$$

3. Shear Moduli of elasticity τ_{xy} along X, Y direction when $\sigma_x = \sigma_y = 0$ & $\tau_{xy} \neq 0$

$$\tau_{XY} = \frac{1}{S_{66}} = \frac{1}{\frac{1}{G_{12}}(C^4+S^4) + 2\left[\frac{2}{E_{11}} + \frac{2}{E_{22}} - \frac{4V_{12}}{E_{11}}\right]S^2C^2} \text{.....3.29}$$

4. Poisons Ratio v_{xy} along X, Y direction

$$v_{XY} = E_X\frac{V_{12}}{E_{11}}(C^4 + S^4) - \left[\frac{1}{E_{11}} + \frac{1}{E_{22}} - \frac{1}{G_{12}}\right]S^2C^2 \text{.....3.30}$$

3.4.2 Stress–Strain Relations of Laminate

A laminate is made of a group of single Plies bonded to each other. These relationships are developed for loads such as shear and axial forces, bending, and twisting moments. The coordinate system used in CLT is shown in Figure 3.11 below.

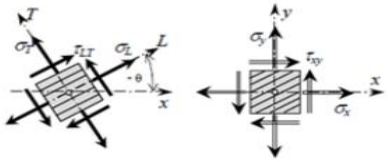

Figure 3.10 Stress resultants of laminated plate along (x,y) & (L,T) Coordinate

knowing the strains at any point along the thickness of the laminate, the stress–strain equation in the global stresses in each single lamina is:

$$\begin{bmatrix}\sigma_x\\ \sigma_y\\ \tau_{xy}\end{bmatrix}=\begin{bmatrix}\bar{Q}_{11} & \bar{Q}_{12} & \bar{Q}_{16}\\ \bar{Q}_{12} & \bar{Q}_{22} & \bar{Q}_{26}\\ \bar{Q}_{16} & \bar{Q}_{26} & \bar{Q}_{66}\end{bmatrix}_k\left[\begin{bmatrix}\varepsilon^0{}_x\\ \varepsilon^0{}_y\\ \gamma^0{}_{xy}\end{bmatrix}+Z\begin{bmatrix}K_x\\ K_y\\ K_{xy}\end{bmatrix}\right], and\ strain\ \begin{bmatrix}\varepsilon_x\\ \varepsilon_y\\ \gamma_{xy}\end{bmatrix}=\begin{bmatrix}\varepsilon^0{}_x\\ \varepsilon^0{}_y\\ \gamma^0{}_{xy}\end{bmatrix}+Z\begin{bmatrix}K_x\\ K_y\\ K_{xy}\end{bmatrix} \quad .....3.31$$

Where "Z" is the distance from the centroidal line and K_x, K_y, and K_{xy} are mid-plane curvatures.

3.4.3 Force and Moment Resultants Related to Midplane Strains and Curvatures

The mid-plane strains and plate curvatures are the unknowns for finding the lamina strains and stresses. The stresses in each lamina can be combined through the laminate thickness to give resultant forces and moments. The forces and moments applied to a laminate will be known, so the mid-plane strains and plate curvatures can then be found. This relationship between the applied loads and the mid-plane strains and curvatures is developed.

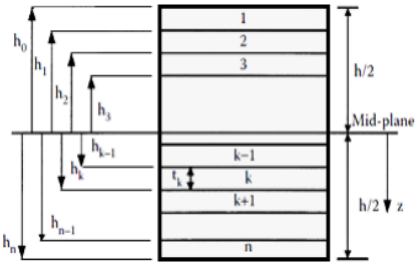

Figure 3.11 Coordinate locations of n plies in a laminate.

Consider a laminate made of n plies shown in Figure 3-12 above. Each ply has a thickness of t_k. Then the thickness of the laminate h is:

$$h=\sum_{K=1}^{n}(t_K) \quad .....3.32$$

The resultant forces and moments can be written in terms of the mid-plane strains and curvatures:

$$\begin{bmatrix}N_X\\ N_Y\\ N_{XY}\\ M_X\\ M_Y\\ M_{XY}\end{bmatrix}=\begin{bmatrix}A_{11} & A_{12} & A_{16} & B_{11} & B_{12} & B_{16}\\ A_{12} & A_{22} & A_{26} & B_{12} & B_{22} & B_{26}\\ A_{16} & A_{26} & A_{66} & B_{16} & B_{26} & B_{66}\\ B_{11} & B_{12} & B_{16} & D_{11} & D_{12} & D_{16}\\ B_{12} & B_{22} & B_{26} & D_{12} & D_{22} & D_{26}\\ B_{16} & B_{26} & B_{66} & D_{16} & D_{26} & D_{66}\end{bmatrix}\begin{Bmatrix}\varepsilon_X^0\\ \varepsilon_Y^0\\ \gamma_{XY}^0\\ K_X\\ K_Y\\ K_{XY}\end{Bmatrix} \quad ..... 3.33$$

Whenever N_x, & N_y, N_{xy}, M_x & M_y, and M_{xy} are (normal force, shear force, bending moments & twisting moments) per unit length, respectively. In short form, it can be written as

$$\begin{bmatrix}N\\ M\end{bmatrix}=\begin{bmatrix}A & B\\ B & D\end{bmatrix}\begin{bmatrix}\varepsilon^0\\ K\end{bmatrix} but\ if\ Inverted, \begin{bmatrix}\varepsilon^0\\ K\end{bmatrix}=\begin{bmatrix}A^* & B^*\\ B^* & D^*\end{bmatrix}\begin{bmatrix}N\\ M\end{bmatrix} \quad ..... 3.34$$

$$when\ \begin{bmatrix}A^* & B^*\\ B^* & D^*\end{bmatrix}=\begin{bmatrix}A & B\\ B & D\end{bmatrix}^{-1}\ and\ [C^*]=[B^*]^T$$

The Extensional Stiffness (A_{ij}), Coupling Stiffness (B_{ij}), and Bending Stiffness (D_{ij}) are given by

$$A_{ij}=\sum_{k=1}^{n}\left[\bar{Q}_{ij}\right]_k(h_k-h_{k-1})\ \ i=1,2,6\ldots andj=1,2,6 \quad .....3.35$$

$$B_{ij}=\frac{1}{2}\sum_{k=1}^{n}\left[\bar{Q}_{ij}\right]_k({h^2}_k-{h^2}_{k-1})\ \ i=1,2,6\ldots andj=1,2,6 \quad .....3.36$$

$$D_{ij}=\frac{1}{3}\sum_{k=1}^{n}\left[\bar{Q}_{ij}\right]_k({h^3}_k-{h^3}_{k-1})\ \ i=1,2,6\ldots andj=1,2,6 \quad .....3.37$$

The extensional stiffness matrix [A] relates resultant in-plane forces to in-plane strains, the coupling stiffness matrix [B] couples the force & moment terms to midplane strains & midplane curvatures,

the bending stiffness matrix [D] relates the resultant bending moments to the plate curvatures. Generally, the stress-strain relationship for the Kth layer laminate composite along (x, y) and along the transformed Longitudinal and Transversal (L, T) axis is shown from fig. 3.12 above is given by:

$$\begin{bmatrix}\sigma_x\\ \sigma_y\\ \tau_{xy}\end{bmatrix}^k = \begin{bmatrix}\bar{Q}_{11} & \bar{Q}_{12} & \bar{Q}_{16}\\ \bar{Q}_{12} & \bar{Q}_{22} & \bar{Q}_{26}\\ \bar{Q}_{16} & \bar{Q}_{26} & \bar{Q}_{66}\end{bmatrix}_k \begin{bmatrix}\varepsilon_x\\ \varepsilon_y\\ \gamma_{xy}\end{bmatrix}^k \text{ and strain } \begin{bmatrix}\varepsilon_x\\ \varepsilon_y\\ \gamma_{xy}\end{bmatrix}^k = \begin{bmatrix}{\varepsilon^0}_x\\ {\varepsilon^0}_y\\ {\gamma^0}_{xy}\end{bmatrix} + Z\begin{bmatrix}\varepsilon_x\\ \varepsilon_y\\ \gamma_{xy}\end{bmatrix} \quad \ldots\ldots\ldots\ldots 3.38$$

$$\begin{bmatrix}\sigma_x\\ \sigma_y\\ \tau_{xy}\end{bmatrix}^k_{(LT)} = [T]_k \begin{bmatrix}\bar{Q}_{11} & \bar{Q}_{12} & \bar{Q}_{16}\\ \bar{Q}_{12} & \bar{Q}_{22} & \bar{Q}_{26}\\ \bar{Q}_{16} & \bar{Q}_{26} & \bar{Q}_{66}\end{bmatrix}_k \begin{bmatrix}\varepsilon_x\\ \varepsilon_y\\ \gamma_{xy}\end{bmatrix}^k \text{ and strain } [\varepsilon]^k{}_{(LT)} = [T]_k[\varepsilon]^k{}_{xy} \ldots\ldots\ldots\ldots 3.39$$

3.4.4 In-Plane and Flexural Modulus of Symmetric Laminate

A laminate is called symmetric if the material, angle, and thickness of plies are the same above and below the midplane (Z=0). For a symmetric laminate, [B] = 0, A_{16} =A_{26} = 0, and it can be shown that [A*] = $[A]^{-1}$ and [D*] = $[D]^{-1}$. Then, Equation 3.33 can be decoupled to give

$$\begin{bmatrix}N_x\\ N_y\\ N_{xy}\end{bmatrix} = \begin{bmatrix}A_{11} & A_{12} & A_{16}\\ A_{12} & A_{22} & A_{26}\\ A_{16} & A_{26} & A_{66}\end{bmatrix}\begin{bmatrix}{\varepsilon^0}_x\\ {\varepsilon^0}_y\\ {\gamma^0}_{xy}\end{bmatrix} or \begin{bmatrix}{\varepsilon^0}_x\\ {\varepsilon^0}_y\\ {\gamma^0}_{xy}\end{bmatrix} = \begin{bmatrix}{A^*}_{11} & {A^*}_{12} & {A^*}_{16}\\ {A^*}_{12} & {A^*}_{22} & {A^*}_{26}\\ {A^*}_{16} & {A^*}_{26} & {A^*}_{66}\end{bmatrix}\begin{bmatrix}N_x\\ N_y\\ N_{xy}\end{bmatrix}$$

$$\begin{bmatrix}M_x\\ M_y\\ M_{xy}\end{bmatrix} = \begin{bmatrix}D_{11} & D_{12} & D_{16}\\ D_{12} & D_{22} & D_{26}\\ D_{16} & D_{26} & D_{66}\end{bmatrix}\begin{bmatrix}{\varepsilon^0}_x\\ {\varepsilon^0}_y\\ {\gamma^0}_{xy}\end{bmatrix} or \begin{bmatrix}{\varepsilon^0}_x\\ {\varepsilon^0}_y\\ {\gamma^0}_{xy}\end{bmatrix} = \begin{bmatrix}{D^*}_{11} & {D^*}_{12} & {D^*}_{16}\\ {D^*}_{12} & {D^*}_{22} & {D^*}_{26}\\ {D^*}_{16} & {D^*}_{26} & {D^*}_{66}\end{bmatrix}\begin{bmatrix}M_x\\ M_y\\ M_{xy}\end{bmatrix} \ldots\ldots\ldots 3.40$$

This shows that the force and moment terms are uncoupled. Thus, if a laminate is subjected only to forces, it will have zero midplane curvatures. Similarly, if it is subjected only to moments, it will have zero midplane strains. The uncoupling between extension and bending in symmetric laminates makes analyzing such laminates simpler.

A. In-plane longitudinal modulus E_x for applying load $N_x \neq 0$, $N_y=0$, $N_{xy}=0$ is $E_x = \frac{1}{hA^*11}$

B. In-plane transverse modulus, E_y, for applying load $N_x=0$, $N_y \neq 0$, $N_{xy}=0$ is $E_y = \frac{1}{hA^*22}$

C. In-plane shear modulus G_{xy} for Appling load $N_x=0$, $N_y=0$, $N_{xy} \neq 0$ is $G_{xy} = \frac{1}{hA^*66}$

D. The effective Poisson's ratio, ν_{xy}, is then defined as: $\nu_{xy} = -A^*_{12}A^*_{11}$

Also, for a symmetric laminate, the coupling matrix [B]= 0; then, from Equation (3.40),

$$\begin{bmatrix}K_X\\ K_Y\\ K_{XY}\end{bmatrix} = \begin{bmatrix}{D^*}_{11} & {D^*}_{12} & {D^*}_{16}\\ {D^*}_{12} & {D^*}_{22} & {D^*}_{26}\\ {D^*}_{16} & {D^*}_{26} & {D^*}_{66}\end{bmatrix}\begin{bmatrix}M_x\\ M_y\\ M_{xy}\end{bmatrix} \ldots\ldots\ldots\ldots 3.41$$

Using the bending compliance matrix [D*] to define effective flexural moduli, first apply $M_x \neq 0$, $M_y= 0$, $M_{xy} = 0$, and then substitute in Equation (3.41), the effective flexural longitudinal modulus, flexural transversal elastic moduli, shear moduli, and Poisson's ratio will be:

$$E_x = \frac{12}{h^3 D^*_{11}}, E_y = \frac{12}{h^3 D^*_{22}}, G_{xy} = \frac{12}{h^3 D^*_{66}} \text{ and } v_{xy} = -\frac{D^*_{12}}{D^*_{11}} \text{ Respectively.}$$

3.4.5 Failure Analysis of Laminate

Material failures occur when a component is subjected to higher stresses & strain values beyond what it can handle. It includes fracture (breakage into two or several parts), buckling, and matrix cracking. So, a laminate will fail under increasing mechanical and thermal loads until all the plies fail. Laminate failure is not catastrophic. If one ply fails, the other ply in the laminate is still capable of taking more loads until all the plies fail.

1) **Tsai-WU Failure Theory**

The Tsai-Wu failure criterion for a lamina is used to predict failure in composite materials, particularly in unidirectional fiber-reinforced laminates. The criterion is formulated to account for the interactions between different stress components in the lamina. The Tsai-Wu is a mode-independent criterion only capable of acknowledging the existence of damage at a certain point of a composite material. It is not capable of identifying if the damage is located in the fibre, matrix, or interlaminar zone(Arruda, Castro and Correia, 2021).

Tsai-Wu's result is more accurate and agrees with the experimental values, because it distinguishes between the tensile and compressive strengths and shows as if it exists a failure surface exists in the stress space. The Tsai–Wu failure criterion is used to predict the first-ply failure load. For orthotropic lamina in a general state of plane stress, for Tsai-Wu failure theory is given by

$$F_1\sigma_1 + F_2\sigma_2 + F_{11}\sigma_1^2 + F_{12}\sigma_2^2 + F_{22}\sigma_2^2 + F_{66}\tau_6^2 \geq 1 \quad \text{.....3.42}$$

where $F_1 = \frac{1}{X_t} - \frac{1}{X_c}$ & $F_2 = \frac{1}{Y_t} - \frac{1}{Y_c}$ Are coefficient for longitudinal strength

$F_{11} = \frac{1}{Y_c Y_t}$ & $F_{22} = \frac{1}{Y_c Y_t}$ are coefficients for transversal strength,

$F_{66} = \frac{1}{\tau^2}$ coefficient for shear & F_{12} is determined experimentally. But if no experimental value, Tsai-Wu recommends using: $F_{12} = -\frac{1}{2}\sqrt{F_{11}F_{22}}$ Magnitude of F_{12} is constrained by an inequality called the stability criterion, i.e.. $F_{11}F_{22} - F^2_{12} > 0$.

When X_t = Allowable tensile stress or strain in longitudinal direction.

X_c = Allowable compression stress or strain in longitudinal direction.

Y_t = Allowable tensile stress or strain in the transverse direction.

Y_c= Allowable compression stress or strain in the transverse direction.

τ = Allowable stress in shear (+ve or -ve shear has the same allowable).

Strength Ratio

If SR>1, then the lamina is safe and the applied stress can be increased by a factor of SR.

If the SR <1, the lamina is unsafe and the applied stress needs to be reduced by a factor of SR.

$$SR = \frac{Ultimate\ stress}{Applid\ stress} > 1 \quad \text{.....3.43}$$

Steps for Laminate Failures

The procedure followed in this paper for finding the first ply and last ply failure load following the fully ply discounted method is.

1. Enter the basic lamina properties E_1, E_2, G_{12} and V_{12}.
2. Compute the reduced ply stiffness [Q] referred to their local axis (principal material axis)
3. Enter the orientation Θ_k, number of layers n, through the thickness coordinate z.
4. Find reduced transformed stiffness matrix$[\bar{Q}]_{xy}$ for each ply of coordinate(x,y)using matrix[Q].
5. Knowing thickness,t_k of each ply, find the coordinate of top & bottom surface h_i when i=l… n.
6. Calculate the laminate stiffness matrices [A], [B], [D], and their compliance matrices.
7. Enter the mechanical loading, $[N]_{xy}$, $[M]_{xy}$.
8. Calculate the midplane strain ε^0_{xy} and curvature $[k]_{xy}$ using the laminate analysis above.
9. Calculate the layer strain $[\varepsilon]^K_{12}$ and stress $[\sigma]^K_{12}$ with reference to the local axis (1, 2) (Longitudinal and Transversal) axis in each layer under the given load.
10. Enter the five-lamina strength and use an appropriate failure theory to find out the strength ratio SR (safety factor) of each of the lamina. Then the minimum SR is the desired one of the laminates.
11. Multiply the minimum strength ratio by the applied load to get the load level of the failure of the first ply. This load is called the First Ply Failure load (FPF).
12. Calculate the laminate strength by applying unit stress in the respective direction.
13. Degrade fully the stiffness of damaged ply(plies). Apply the actual load level of the previous failure.
14. Go to step 10 to find the strength ratio (SR) in the undamaged plies. If the SR>1, multiply the SR by the applied load to get the load level of the next ply failure, and go to the next step
15. If SR< 1, Stiffness & Strength properties of all damaged plies reduce & go back to step 13.
16. Repeat the preceding steps until all plies in the laminate have failed. The load at which all the plies in the laminate have failed is called the last ply failure.

3.5 Design And Analysis Of Laminated Bumper Beam

A bumper is a structure, which attached to the front and rear of the vehicle. The primary purpose of the bumper is to absorb the minor impact collision, which avoids minor repair costs. But later on, with the development of technology, the bumper is used to reduce pedestrian injuries and protect passengers. A beam is a structural member that is subjected primarily to transverse loads & negligible axial loads. Bumper Beam is a type of beam fixed to the front chassis to absorb impact forces caused by collisions. Its energy absorption capability can be affected by various parameters like Curvature of the front chassis, Stress concentration, Material properties (volume ratio and orientation), Cross-section, and Thickness. A strong bond between fiber and matrix is required for structural applications, whereas a weak and ductile interface increases the composite toughness and is more suitable for impact applications (Chinnasamy and Periasamy, 2021). In this project, a front bumper made of Glass, Sisal, wool fiber, and epoxy reinforced composite materials is studied through crash simulation analysis to determine the stress, kinetic energy, potential energy, and strain energy using MATLAB and finite element methods.

3.5.1 Input Parameters & Material Properties of Bumper Beam

A). Dimensions and Input Parameters of Bumper Beam

Performance standards for bumpers vary by country. According to international safety regulations, initially established as European standards and now widely adopted outside of America, a car's safety systems must operate effectively after a straight-on pendulum or moving-barrier impact at speeds of 4 km/h (2.5 mph) for the front and rear corners, and 2.5 km/h (1.6 mph) at a height of 45.5 cm (18 in), regardless of whether the vehicle is loaded or unloaded. In North America, the Federal Motor Vehicle Safety Standards (FMVSS) and Canadian Motor Vehicle Safety Standards (CMVSS) require compliance with 8 km/h impacts(Reddy, no date)(Shok, Abu and Aidu, 2016). The dimensions of the bumper beam have been derived from measurements of an existing steel bumper, with some parameters referenced from international standards such as ASTM A-370 for Impact Testing(Dange, Buktar and Raykar, 2015). All dimensions, except for the thickness of the composite bumper, are assumed to be the same as those of the mild steel bumper (with chromium coating) used as a mold for fabrication. Below are some of the bumper beam's dimensions(Buba, Bello and Jatau, 2023).

Table 3.8 Dimensions and Some Input Parameters of Bumper Beam

Dimensions of Bumper Beam	Symbols	Values	
Material Type	-	Mild Steel	Composite
Cross Section	A	C–type	C–type
Tensile strength	σ_t	460Mpa	114.07Mpa
Density of material	ρ	7800 kg/m^3	1359Kg/m^3
Total Length	L_t	2.055m	2.055m
Effective Length	L_e	0.975m	0.975m
Height above ground	H	45.5cm	45.5cm
Total breath(width)	B	0.172m	0.172m
Effective breath	B	0.078m	0.078m
Effective Thickness	T	2mm	5.82mm
Effective Surface Area	A_e	0.219m^2	0.353m^2
Weight of Bumper Beam	W_b	5.16Kg	3.8Kg
Weight of Car (Impactor)	W_I	1322Kg	1322Kg
Assumed time of Collision	T	0.1s	0.1s
Total cost	C	32000	14000

Effective Length is a Length mostly subjected to collision which is 70% of total length.

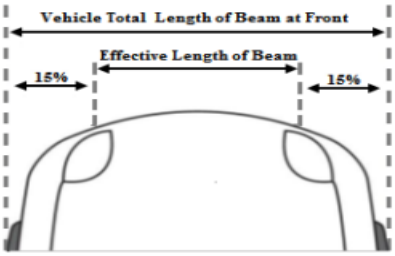

Figure 3.12 Percent Overlap Based on Vehicle Width from Top View of Beam at Front Axl

A) Material Properties of Bumper Beam

Materials used for bumper beam are a hybrid of Glass, Sisal and wool fiber, and epoxy reinforced composite material. The property of the materials is taken either experimentally or from Design Data Books. The most common material properties of composite & steel materials used to fabricate the Bumper Beam are listed below.

Table 3.9 Material properties of composite

Moduli parameters	Symbol	Glass/epoxy	Sisal/epoxy	Wool/epoxy
Volume ratio	V_f	0.18	0.18	0.09
Density	ρ (g/cm3)	1.5 2	1.27	1.3
Longitudinal modulus	E_1 (MPa)	16370	5930	3680
Transversal modulus	E_2 (MPa)	3480	3070	2950
Shear modulus	G_{12} (MPa)	1410	1240	1140
Longitudinal tensile strain	e_L(mm)	2	1.95	3.4
Poissons ratio	μ_{12}	0.34	0.345	0.354
Longitudinal tension	X_t (MPa)	499.2	148.2	60
Longitudinal compression	X_c (MPa)	327.4	138.4	68.65
Transverse tension	Y_t (MPa)	68	59	49.1
Transverse compression	Y_c (MPa)	46.7	41.3	34.55
Shear strength	τ_{12} (MPa)	35.4	28.38	29.58

3.5.2. Design Calculation of Bumper Beam

Considering the Bumper beam is fixed at both end & subjected to Uniformly Distributed loads because of Collison between two vehicles or between one vehicle and rigid body then the UDL cause internal shear forces & bending moments in the beams as shown in (Figure 3-15A) Again, these internal shear forces and bending moments cause longitudinal axial stresses and shear stresses in the cross-section (Figure 3-15B) below.

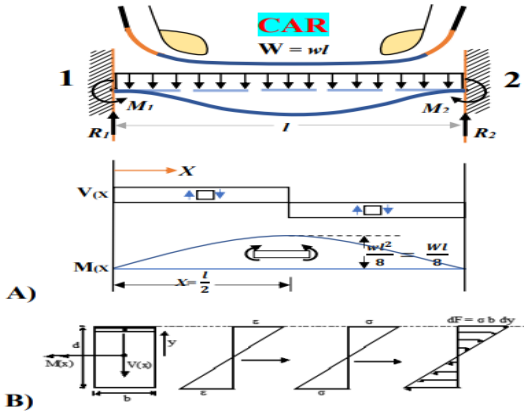

Figure 3.13 Internal shear force & bending moment diagrams for transversely loaded beams(A) Longitudinal axial stresses caused by internal bending moment(B).

Curvature$\emptyset = \frac{\varepsilon}{d/2}$, $F = \int_{-d/2}^{+d/2} \sigma b \, dy$, $M = \int_{-d/2}^{+d/2} \sigma b \, dy \; y$

Steps followed for Design Calculation of the bumper beam are:

I. Calculate the factored loads (Shear, Impact & Moment...)

Having mass of impactor (mass of car) m_{im}, initial Speed u_{im}, time of collision 't', etc., then

- Reactions $R_1 = R_2 = \frac{W}{2}$ and Bending momentums M1 = M2 = $\frac{WL}{12}$
- Ultimate load, P = W = $\frac{F}{A} = \frac{M_{im} \times a}{A} = \frac{M_{im} \times v_{im}}{A_t}$ Acting on beam (UDL)
- Impact (KE) Energy, E = ½ $M_{im} v^2_{im}$
- Impact strength, I = $\frac{E}{AK}$, K is aspect ratio = 0.5 for Glass & most natural fibers.
- Shear: V = $\frac{W}{2}(1 - \frac{2X}{L}) \Rightarrow V_1 = \frac{WL}{2}$ @ x = 0 and V_2 = - $\frac{WL}{2}$ @ x = l
- Ultimate momentum = $M_u = \frac{WL^2}{12}$
- Max +Mb = $\frac{W}{2}(X - X - \frac{X^2}{L} - \frac{L}{6}) = \frac{WL}{24}$ @ x = $\frac{L}{2}$ and Max -Mb = - $\frac{WL}{12}$ @ 1 & 2

Since the composite is needed to replace the strength of conventional materials like steel, the momentum for the steel and composite bumper is assumed to be the same. The bending moment equation of the Steel bumper Beam is $M = \frac{\sigma s(I)}{Y}$.

II. Select the C-channel shape and calculate the Thickness of the Composite Beam.

The selected cross-section for bumper beam is a C-Channel having three sections with its moment of inertia I_1, I_2, I_3 & its total value of I = I_1+ I_2 +I_3 = bt^3 /12 and Y= t/2.

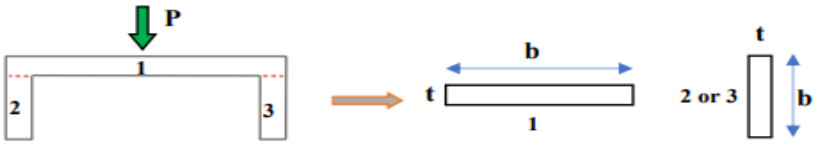

Figure 3.14 Cross-section of bumper beam

$I_1 = 0.172 \times 0.002^3 / 12 = 1.146 \times 10^{-10}\ m^4$
$I_2 = 0.078 \times 0.002^3 / 12 = 5.2 \times 10^{-11}\ m^4$
$I_3 = 0.078 \times 0.002^3 / 12 = 5.2 \times 10^{-11}\ m^4$
$I = I_1 + I_2 + I_3 = 2.186 \times 10^{-10}\ m^4$
$M = \frac{\sigma steel\ (I)}{Y} = \frac{460Mpa\ (2.186x\ 10-10m4\ )}{0.002m/2} = 100.556Nm$

The thickness of the composite bumper can be determined from the bending moment of steel equation individually for t_1, t_2, and t_3 of each section to get Average thickness (t) = $(t_1+t_2+t_3)/3$.

$\frac{M}{I_1} = \frac{\sigma_{comp}}{Y_1} = \frac{100.556Nm}{\frac{0.172m \times {t_1}^3}{12}} = \frac{(181.833Mpa)}{\frac{t_1}{2}}, \rightarrow t_1 = 4.41mm$, when $I_1 = \frac{b{t_1}^3}{12}$, $Y_1 = \frac{t_1}{2}$

$\frac{M}{I_2} = \frac{\sigma_{comp}}{Y_2} = \frac{100.556Nm}{\frac{0.078m \times {t_2}^3}{12}} = \frac{(181.833Mpa)}{\frac{t_2}{2}}, \rightarrow t_2 = 6.52mm = t_3$

$t_t = \frac{t_1+t_2+t_3}{3} = 5.82mm$ total thickness of composite laminate

Therefore, since the average thickness single ply of sisal, wool & glass is 1.164mm, then five layers (GSWSG) are required for fabricating the composite bumper Beam.

III. Check the Momentums of the Bumper Beam

The Momentum capacity of the selected Cross section (C-channel) $\phi_b M_n > M_u$ (Note $\phi_b = 0.9$)

- $M_p = \sigma_y * A/2 * t$, so that $\phi_b M_p = 0.9\ Z * \sigma_y$ when $Z = A/2 * t$
- $\phi_b M_n$ = Moment capacity = C_b x ($\phi_b M_n$ for the case with uniform moment) $\leq \phi_b M_p$
- Select $\phi_b M_n$ and C_b =1.0 for channels
- $\phi_b M_n$ is > M_u & $\leq \phi_b M_p$ so it is **OK**

IV. Check deflection at a given load

The maximum deflection of the designed beam is checked at the given Uniformly Distributed loads & must be less than the Maximum allowable deflection.

- Uniform Distributed load = W
- Deflection due to W is $\Delta d = \frac{5WL^4}{384EI}$ when $I = \frac{bh^3}{12}$or
- $\Delta d = \frac{1}{24}\frac{WX^2}{EIL}(2LX - X^2 - L^2)$
- $\Delta d\ max = \frac{1}{384}\frac{WL^3}{EI}$ @ $x = \frac{L}{2}$

The maximum allowable total deflections due to different constructions are.

Type	Plastered floor construction	Unplastered floor construction	Unplastered roof construction
Δ_{max}	L/360	L/240	L/180

Assuming plastered floor construction, Δmax = L/360.
Therefore, $\Delta d < \Delta_{max}$ **OK**

V. Check for local buckling for channel section, see Table 3.10 below

To design all beam sections, it is needed to be compact from a local buckling standpoint. If all elements of the cross-section have $\lambda \leq \lambda p$ then it is called a Compact section.

- $\lambda = \frac{b_f}{t_f}$ Corresponding $\lambda_p = 0.38\sqrt{\frac{E}{F_Y}}$
- Therefore, if $\lambda < \lambda_p$ - compact flange
- $\lambda = \frac{h}{t_w}$ Corresponding $\lambda_p = 3.76\sqrt{\frac{E}{F_Y}}$
- Therefore, if $\lambda < \lambda_p$ - compact web

If it is a Compact section, then it is – **OK**

Table 3.10 λ, λ p, and λ r values for the individual elements of various cross-sections

Section	Plate element	λ	λ_p	λ_r
Wide-flange	Flange	$b_f/2t_f$	$0.38\sqrt{E/F_Y}$	$1.0\sqrt{E/F_Y}$
	Web	h/t_w	$3.76\sqrt{E/F_Y}$	$5.7\sqrt{E/F_Y}$
Chennel	**Flange**	$\mathbf{b_f/t_f}$	$\mathbf{0.38\sqrt{E/F_Y}}$	$\mathbf{1.0\sqrt{E/F_Y}}$
	Web	$\mathbf{h/t_w}$	$\mathbf{3.67\sqrt{E/F_Y}}$	$\mathbf{5.7\sqrt{E/F_Y}}$
Square or Rect. Box	Flange	(b-3t)/t	$1.12\sqrt{E/F_Y}$	$1.4\sqrt{E/F_Y}$
	Web	(b-3t)/t	$2.42\sqrt{E/F_Y}$	$5.7\sqrt{E/F_Y}$

When: P – Impact Load (Pressure) on bumper is considered as Uniformly Distributed
I – Impact strength of the specimen in J/sq.cm
M_p – Plastic moment capacity, M_u – Ultimate Moment
Δ_d –Deflection, λ –Buckling and
E –Modulus of elasticity
A–Cross-sectional area, I–Moment of inertia (m^4) & t–thickness of bumper (m).

3.5.3. Bending Analysis of Composite Beam

Uses to find the deflection and stresses (Local or Global) in a symmetric beam made of composite materials.

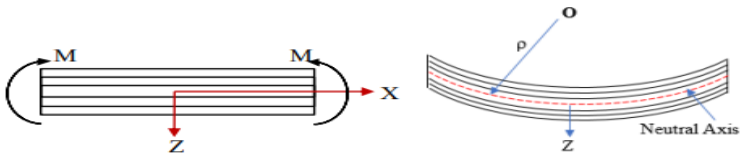

Figure 3.15 Bending of a beam and Curvature of a bended beam

The beam is symmetric so the loads & moments are decoupled in Equation (3:45) to give

$$\begin{bmatrix} M_X \\ M_Y \\ M_{XY} \end{bmatrix} = [D] \begin{bmatrix} K_X \\ K_Y \\ K_{XY} \end{bmatrix} \gg \begin{bmatrix} K_X \\ K_Y \\ K_{XY} \end{bmatrix} = [D]^{-1} \begin{bmatrix} M_X \\ M_Y \\ M_{XY} \end{bmatrix} \text{..... 3.44}$$

Now, if bending is only taking place in the x-direction, then My = 0, Mxy = 0

$\begin{bmatrix} K_X \\ K_Y \\ K_{XY} \end{bmatrix} = [D]^{-1} \begin{bmatrix} M_X \\ 0 \\ 0 \end{bmatrix}$ Then, from this, $K_x = D^*_{11} M_x$, $K_y = D^*_{12} M_x$, and $K_{xy} = D^*_{16} M_x$

if we have a narrow beam — that is, the length to width ratio (L/b) is sufficiently high, we can assume that midplane deflection ω0 = ω0(x). Then the midplane curvature is given by

$$K_x = \frac{d^2\omega_0}{dx^2} = D^*_{11} M_x = -\frac{M_x b}{E_x I} \text{..... 3.45}$$

Therefore, from Equation above equation, we get

1. **Maximum Deflection δ for Isotropic Beam**

$$\delta = \frac{5qL^4}{384E_xI} \text{ .....3.46}$$

When Ex, = $\frac{12}{h^3 D^*_{11}}$, $I = \frac{bh^3}{12}$ and M = M_x b

2. **The local stresses in each ply are**

$$\begin{bmatrix} \sigma_1 \\ \sigma_2 \\ \tau_{12} \end{bmatrix}^K = [Q]_K \begin{bmatrix} \varepsilon_1 \\ \varepsilon_2 \\ \gamma_{12} \end{bmatrix}^K When \begin{bmatrix} \varepsilon_1 \\ \varepsilon_2 \\ \gamma_{12} \end{bmatrix}^K = [R][T][R]^{-1} \begin{bmatrix} \varepsilon_1 \\ \varepsilon_2 \\ \gamma_{12} \end{bmatrix} \text{.....3.47}$$

3. **The global stresses in each ply are**

$$\begin{bmatrix} \sigma_x \\ \sigma_y \\ \tau_{xy} \end{bmatrix}^K = [T]^{-1}{}_K \begin{bmatrix} \sigma_1 \\ \sigma_2 \\ \tau_{12} \end{bmatrix}^K \text{..... 3.48}$$

3.5.4. Impact Analysis of Composite Bumper Beam Using Genetic Algorithm

A genetic algorithm is a high-performance finite element pre-processor.This approach helps to identify optimal design configurations that enhance impact resistance while adhering to safety and performance standards. The integration of FEA and GA allows for a robust analysis of complex composite materials under dynamic loading conditions. Steps to Analyze Impact of Composite Bumper Beam Using GA;

1. **Define the Objective**

Identify the primary goal of the analysis. Common objectives include:

- Minimizing weight, Maximizing energy absorption, Optimizing material distribution

2. **Formulate the Objective Function**

The objective function should quantify the goal. The goal is to minimize the mass of the bumper beam while ensuring it meets impact strength requirements. The function could be defined as:

- Objective Function (mass)=Volume×Density
  Where: **Volume** is calculated based on the geometry of the bumper beam.
  Density is based on the composite materials used.

3. **Identify Design Variables**

Determine the design variables that will be optimized. For a composite bumper beam, these might include:

- Thickness of different layers (glass, sisal, wool)
- Fiber orientation(GSWSG)
- Material composition ratios(fiber volum ratio is 45%, matrix volume ratio is 55%)

4. **Set Constraints**

Define constraints to ensure that the bumper meets safety and performance standards. Constraints may include:

- Maximum allowable deflection under impact
- Minimum energy absorption required
- Material strength limits (tensile, compressive, shear)

5. **Create the Genetic Algorithm Model**

Using a programming environment, MATLAB, set up the GA model:

- **Population Size**: Define how many individuals (solutions) will be evaluated.
- **Selection Method**: Choose a method for selecting the best individuals (e.g., roulette wheel, tournament selection).
- **Crossover and Mutation**: Define how new individuals will be generated from existing ones.
- **Termination Criteria**: Set criteria for when to stop the GA (e.g., maximum generations, convergence threshold).

6. **Implement the GA**

Write the GA code, incorporating the objective function and constraints. Here's a simplified structure in pseudo-code:

7. **Evaluate and Analyze Results**

Once the GA has run, analyze the results:

- Review the best solution found by the GA.
- Evaluate how well it meets the constraints and objectives.
- Perform sensitivity analysis to see how changes in design variables affect performance.

8. **Validation**

Validate the results through:

- Finite Element Analysis (FEA) to simulate impact and verify the performance of the optimized design.
- Experimental testing on physical prototypes to ensure real-world performance aligns with predictions.

3.6 Design optimization of the Composite bumper beam

It is, a process of achieving a maximized objective with a given variables under constrained parameters. Steps for the Design optimization process are listed below:

1. Analysis Type: Static, Dynamic, Normal Mode, and Bulking….

2. Optimization Type: Sizing, Shape, Topology, and multi-objective optimization.

3. Design Variables: what can be varied or changed.

- No of plies, thickness of plies, and Ply orientation, Material Property…etc.

4. Design Constraints: What are the limits on the Design response?

- Failure indices, Strength ratio and Weight, Stress/Strain, Displacement, etc.

5. Design Objective: what is wanted to maximize or minimize.

- Minimize weight, thickness, etc., and Maximize Strength, stiffness, etc.

Generally, even though there are a lot of optimization techniques, the design requirement for the hybrid bumper beam is to minimize the weight undergo minimize cost, while maintaining impact performances and maximizing the stiffness. The weight of the bumper beam depends on the material and thickness of the bumper beam parts. The mass of the bumper beam m_b can be calculated as

$$m_b=\rho_b \sum_{i=1}^{n} (A_{surface,i} * t_{part,i}) \quad \text{..... 3.49}$$

Where ρ_b is density, n is the number of bumper beam parts, A is area, and t_{part} is the thickness of the part, respectively.

3.7 FEA for Validation

Finite Element Analysis (FEA) was used to simulate impact and verify the performance of the optimized design, and was analyzed by using ABAQUS for validation. It ensures that the optimized outcomes produced by the genetic algorithm are reliable and consistent with real-world behavior modeled in ABAQUS.

3.7.1 Define Geometry and Material Properties (model)

Model the bumper beam (dimensions: thickness, length, width). Assign the material properties for each component (Density, Elastic properties, and Strength properties): Figure 3-13 illustrates the structural model of the glass, sisal, and wool fiber and epoxy laminate, along with the stacking sequence of the ply laminate. Based on the results from the genetic algorithm, it is designed for the optimized dimension and optimized ply orientation, which is (90°,15°, 0°,15°, 90°).

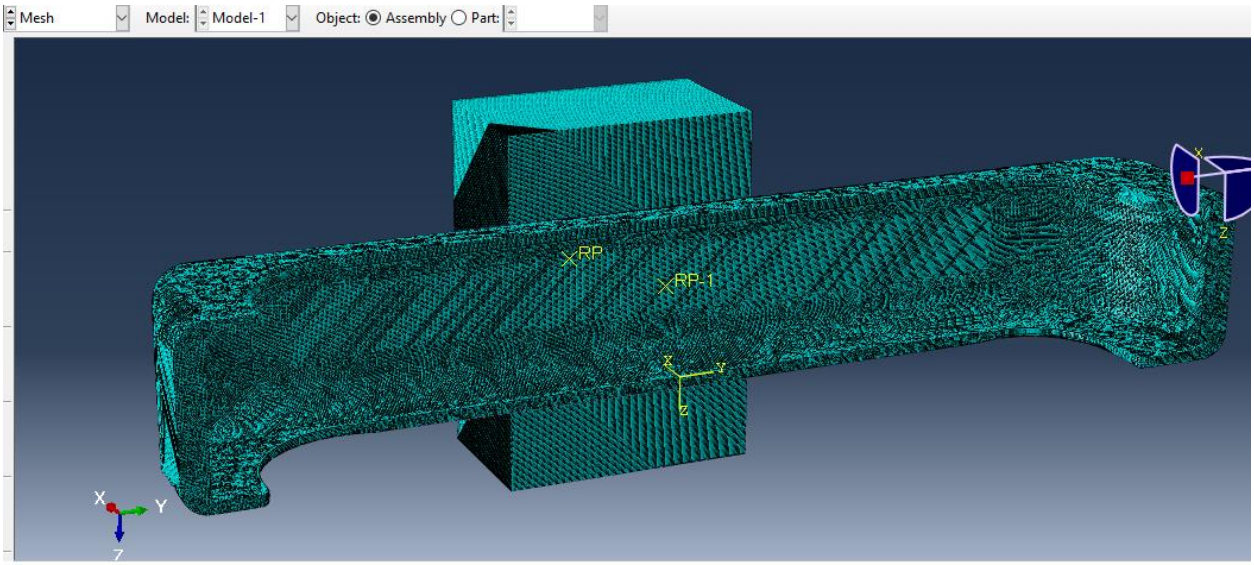

Figure 3.16Meshing of composite bumper

4 RESULT AND DISCUSSION

4.1 EXPERIMENTAL RESULT OF LAMINATED COMPOSITE

The experimental mechanical and physical property test has been conducted for Glass, Sisal, and wool fiber, and epoxy reinforced laminate composite sample, which is limited only to mechanical properties, tensile, impact, flexural, compression, and for physical properties, water absorption, and density test results to select the laminate with appropriate properties.

Table 4.1:physical and mechanical properties of laminated composites

Sample	Strength					Water absorption (%)	Density g/cm^3	
	Tensile (Mpa)	Ultimate tensile (Mpa)	Compressive (MPa)	Impact (KJ/m^2)	Flexural (Mpa)		Theortical	Actual
GSWSG	114.07	145.92	92.13	112.5	1270.6	3	1.359	1.35
SGWGS	85.8	105.86	72.75	87.5	704.1	9	1.359	1.43
WWWWW	105.4	127.27	84.62	50	1753.1	4	1.382	1.26
SSSSS	102.5	145.38	90.37	80	1284	11	1.42	1.18

4.1.1 Tensile Strength of the Bumper

The tensile strength of the composite bumper was tested, and the ultimate tensile strength of each specimen was computed. And the maximum average value of 145.92MPa was obtained as given in Table 4.2. The major purpose of the test is to determine the ultimate tensile stress at which the composite bumper will fail. This means that if the bumper is subjected to a tensile stress beyond 114.07MPa, it will fail.

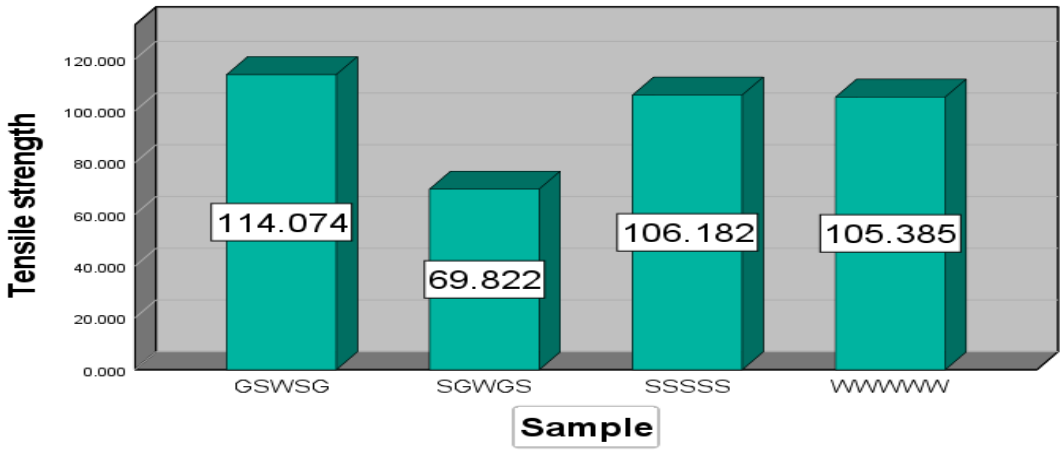

Figure 4.1Graphical representation of tensile strength.

4.1.2 Compressive Strength of the Bumper

The compressive strength of the bumper was tested, and the average value in Table 4-1 was 92.133MPa, taken as the ultimate compressive strength at the critical condition. This means that if

the composite is stressed beyond this value, it will fail. The failure of the composite was characterized by brittle fracture.

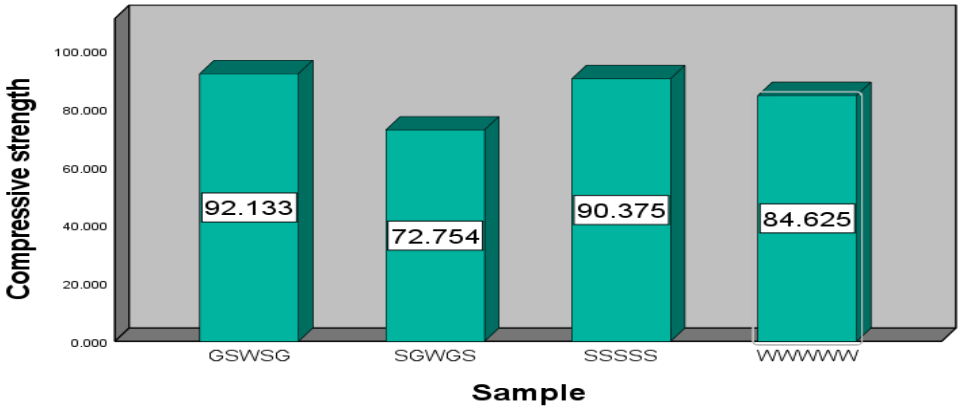

Figure 4.2 Graphical representation of compressive strength

4.1.3 Flexural Strength of bumper

The flexural strength test was carried out on the composite bumper at different points and lengths of span. The result computed, given in Table 4-1, indicated that the bumper can withstand maximum stress up to 1270.6MPa before failure. That shows that with an increase in the size of the specimen, the flexibility increases, hence the flexural strength, which applies to the composite bumper.

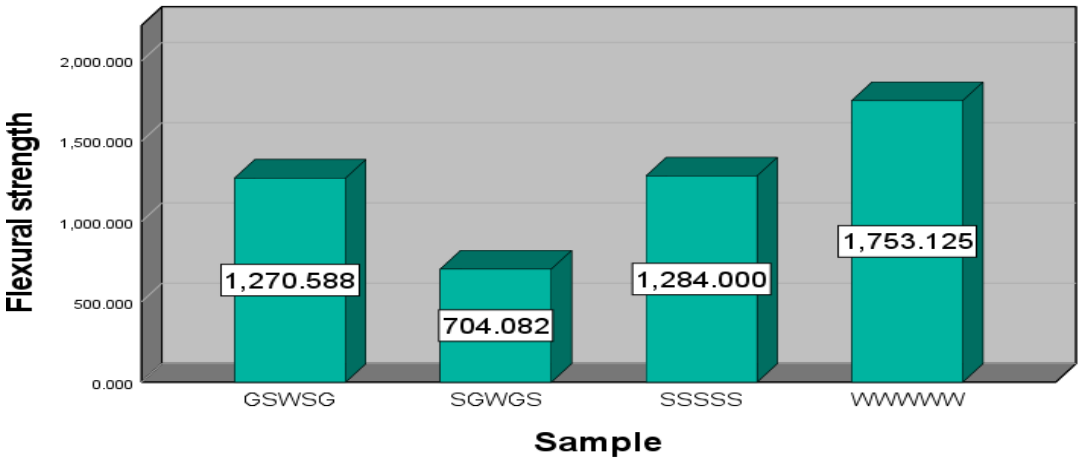

Figure 4.3 Graphical representation of flexural strength

4.1.4 Impact strength of bumper

Impact Energy of Bumper Table 4-1 showed the impact energy absorbed per unit area by the bumper and was found to be 112.5KJ/m^2 at an impact velocity of 3.5m/s (12.6km/hr). The result was also interpreted in a graph figure below for the behavior of internal stresses the specimen undergoes. The result obtained is higher than the recommended value of $49.34 KJ/m^2$ at a speed of 8km/hr. It can be inferred that the bumper will withstand the impact of the vehicle at 8kh/hr without damage.

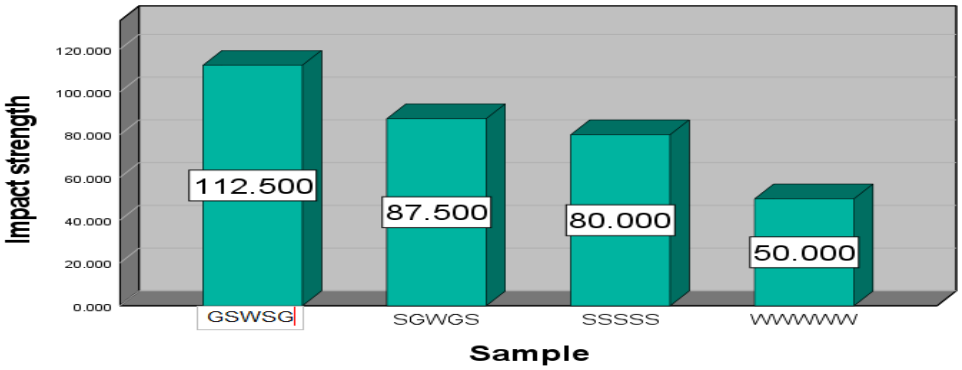

Figure 4.4 Graphical representation of impact strength

4.1.5 Density of Bumper

The average density of the composite bumper in table4-1 was found to be 1.348kg/m3, which was less than the theoretical density of 1.359kg/m3. The experimental density is less than the theoretical density of the fabricated composite bumper because of the void content. The void content affects the strength of the composite bumper; therefore, a roller brush is suggested to be used in applying the resin to reduce the void content in subsequent production.

Void Content of composite Bumper

The percentage void content in the glass/ sisal/wool fiber-reinforced epoxy composite bumper was calculated and found to be 0.6%. The value shows that it is less than the recommended value of 1% for a good bonded composite. Therefore, the void content is negligible, and the composite bumper is within the standard quality.

4.1.6 Water Absorption of Bumper

The percentage of water absorbed by the composite bumper was found to be 3% when it was soaked in water for 360 hours, as shown in table4-1. This means that if the bumper is exposed to continuous rain for 360 hours, its weight will increase by 0.5%. Interestingly, when the bumper was exposed to the sun at an average temperature for 12 hours, the absorbed moisture dried off. Therefore, there is a need to oven-dry the bumper after production to reduce the moisture content of the composite bumper.

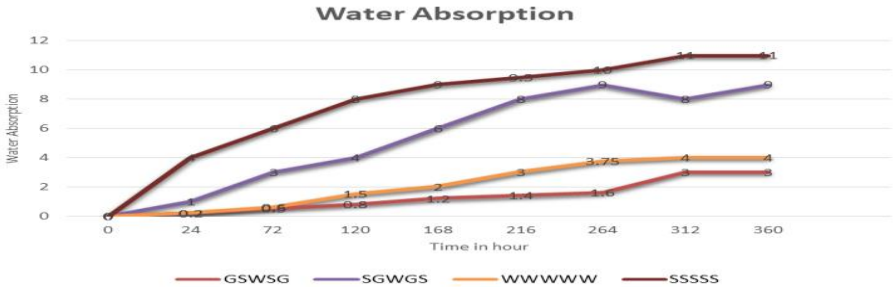

Figure 4.5 Graphical representation of water absorption

4.2 Design Calculation of Composite Bumper Beam

Input data: Mass of the vehicle =1322 kg

Average mass of 5 persons =350 kg

Total mass of vehicle =1322+350 =1672 kg

Speed of the car =8km/hour =2.22 m/s.

Assume this car is hitting another identical one, and it will stop in 0.1 seconds.

Deceleration of the car =(u+v) / t = (2.22-0)/0.1 = 22.2 m/s^2.

where, v= final velocity of car in m/s, u = initial velocity ofcar in m/s, t=time after which vehicle stopped inseconds.

Force acted during collision =m*a =1672*22.2 = 37.12 KN

Where, m= mass of car in kg , a = acceleration of car in m/s^2

Smallest area of impact on the bumper =Le*B=0.975*0.172m^2 =0.1677m^2

Pressure acted on the bumper =F/A =37.12/0.1677=221.35KN/m^2(Reddy, no date).

I. Calculate the factored loads (Shear, Impact & Moment...)

Having mass of impactor (mass of car) m_{im}, initial Speed u_{im}, time of collision 't', etc., then

- Reactions $R_1 = R_2 = \frac{W}{2} = 110.67\text{KN/m}^2$
- Bending momentums M1 = M2 = $\frac{WL}{12} = 37.9KN/m$
- Ultimate load, P = W = $\frac{F}{A} = \frac{M_{im}\times a}{A} = \frac{M_{im}\times v_{im}}{A_t} = 221.35\text{KN/m}^2$ At acting on beam (UDL)
- Impact (KE) Energy, E = ½ $M_{im}v^2{}_{im} = 4120.14\text{J}$
- Impact strength, I = $\frac{E}{AK}$, K is aspect ratio = 0.5 for Glass & most natural fibers. or energy absorbed per unit area I = $\frac{E}{AK} = 49.34KJ/\text{m}^2$
- Shear: V = $\frac{W}{2}(1-\frac{2X}{L}) \Rightarrow V_1 = \frac{WL}{2} = 227.44KN/\text{m}^2$ @ x = 0 and
  $V_2 = -\frac{WL}{2} = -227.44KN/\text{m}^2$ @ x = l
- Ultimate momentum = $M_u = \frac{WL^2}{12} = 77.89KN$
- Max +Mb = $\frac{W}{2}(X - X - \frac{X^2}{L} - \frac{L}{6}) = \frac{WL}{24} = 18.95KN/m$ @ x = $\frac{L}{2}$ and
  Max -Mb = $-\frac{WL}{12} = -37.9KN/m$ @ 1 & 2

II. Check the momenta of the Bumper Beam

The Momentum capacity of the selected Cross section (C-channel) $\phi_b M_n > M_u$ (Note $\phi_b = 0.9$), $\sigma_{y=}$94.2Mpa

- $M_p = \sigma_y * A/2 * t$, so that $\phi_b M_p = 0.9\ Z * \sigma_y$ =39.1KNm when $Z = A/2 * t$
- $\phi_b M_n$ = Moment capacity = C_b x ($\phi_b M_n$ for the case with uniform moment) ≤ $\phi_b M_p$
- Select $\phi_b M_n$ and C_b =1.0 for channels
- $\phi_b M_n$ is > M_u & ≤ $\phi_b M_p$ so it is **OK**

III. Check deflection at a given load

The maximum deflection of the designed beam is checked at the given Uniformly Distributed loads & must be less than the Maximum allowable deflection.

- Uniform Distributed load = W=221.35KN/m^2
- Deflection due to W is $\Delta d = \frac{5WL^4}{384EI} = 18.94m$ when $I = \frac{bh^3}{12} = 2.186\text{x}10^{-10}$ m4 and E=12.45Gpa
- $\Delta d = \frac{1}{24}\frac{WX^2}{EIL}(2LX - X^2 - L^2)$
- Δd max = $\frac{1}{384}\frac{WL^3}{EI}$ =14.44m@ x = $\frac{L}{2}$, Yes- OK

4.3 Impact Analysis Optimized Result Of The Composite Bumper Beam Using Genetic Algorithm

To obtain the optimized laminated bumper beam, the thickness of the laminate was first solved using MATLAB software. This was done using the results of the classic laminate theory, which was used in the structural design of the composite. The weight of the bumper was minimized based on the thickness of the structure obtained in the design by taking into account the properties of the laminated hybrid composite using MATLAB. The density of fibers obtained from the experiment was used to determine the mass, and finally, the equation can generalize the minimized mass of the laminate composite bumper beam.

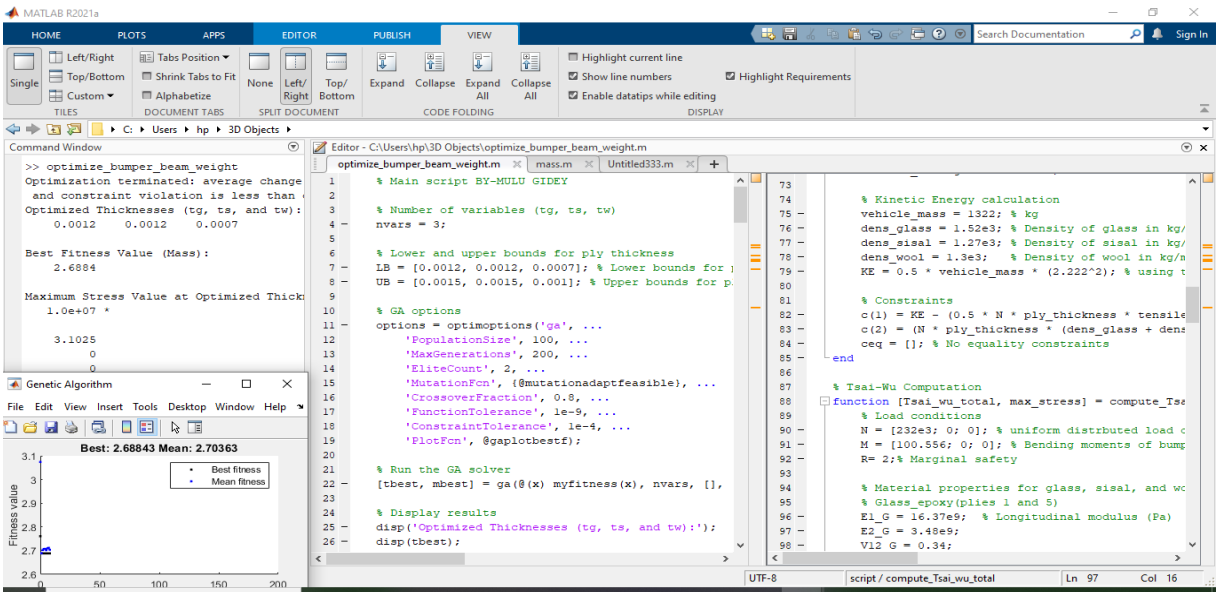

Figure 4.6 MATLAB program of composite bumper beam using GA

4.4 FEA result

4.4.1 Stress distribution of composite bumper beam

The stress distribution of Glass/Sisal/Wool fiber reinforced epoxy resin laminate composite front bumper beam can be observed as shown in the figure below, and the maximum stress obtained is 31 N/mm2 at the center of the Beam, which is below the yield strength of the material that showing that it is safe.

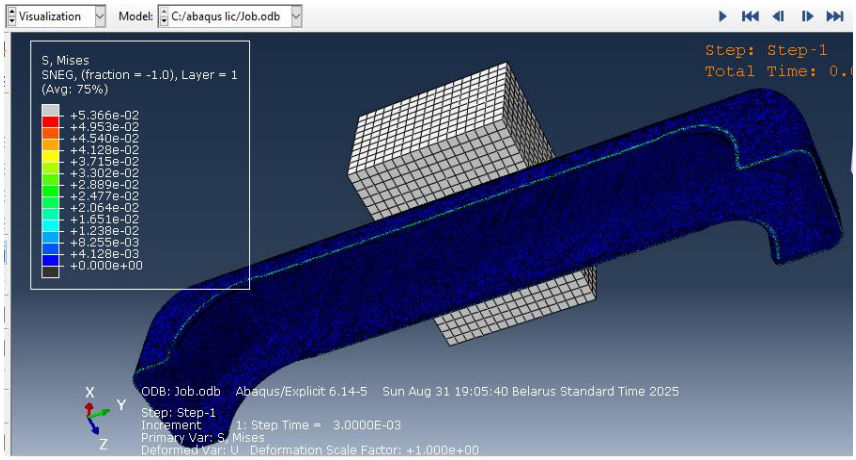

Figure 4.7 Optimized Composite Stress (Von Mises Stress)

4.4.2 Element stress of the composite bumper

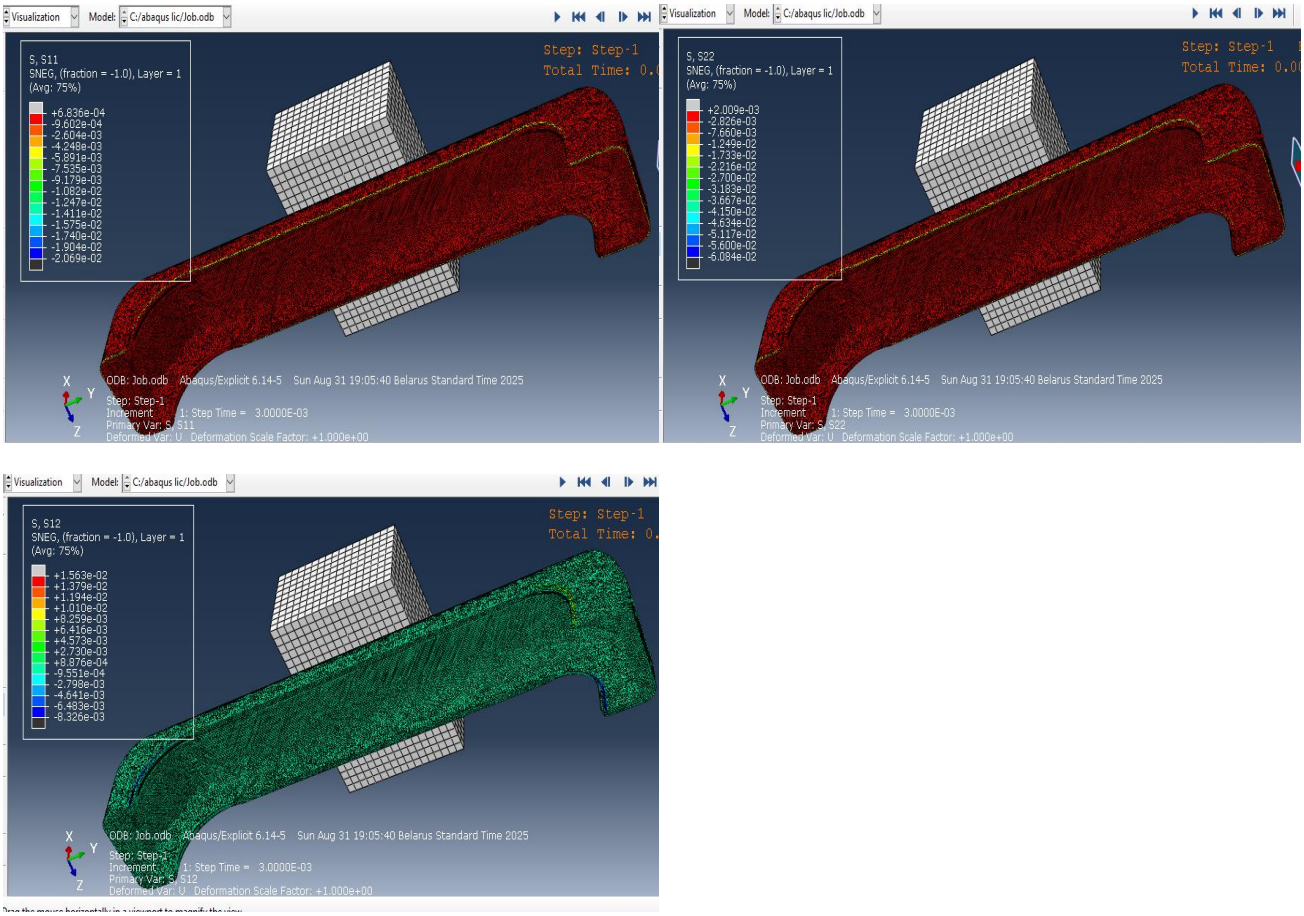

Figure 4.8 Optimized Element stress of composite bumper

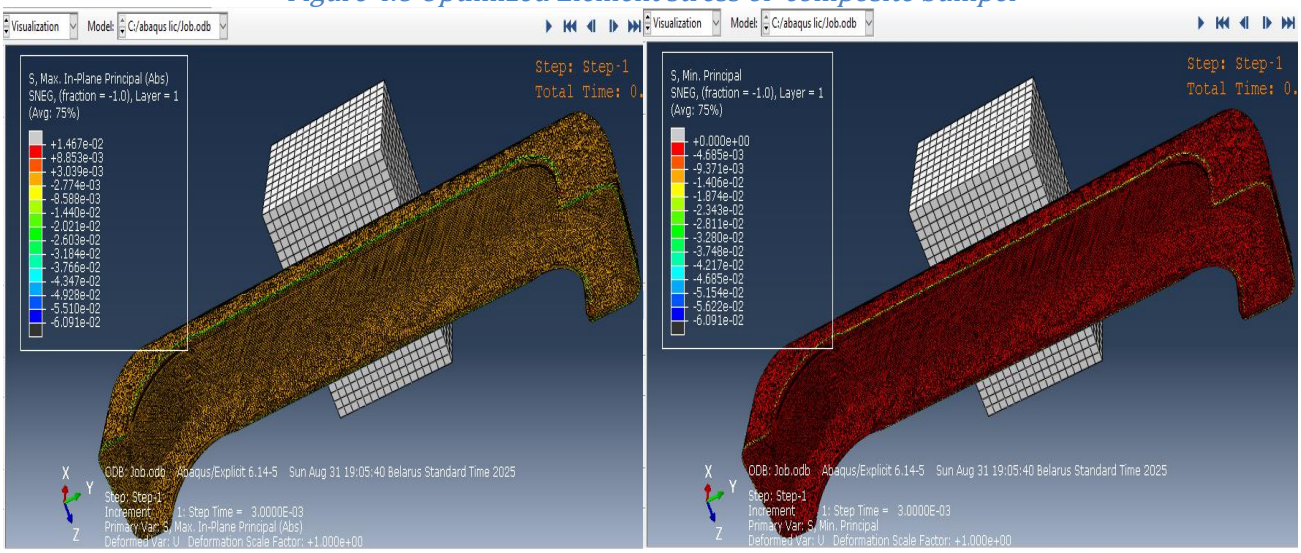

Figure 4.9 Max and min principal Plane stress of Composite Bumper Beam

4.4.3 Deformation of the composite bumper beam

Then /the Deflection for Glass/Sisal/Wool fiber reinforced epoxy resin Laminate Composite Material can be observed as shown in the Figure below, and the maximum deflection obtained is 89 mm.

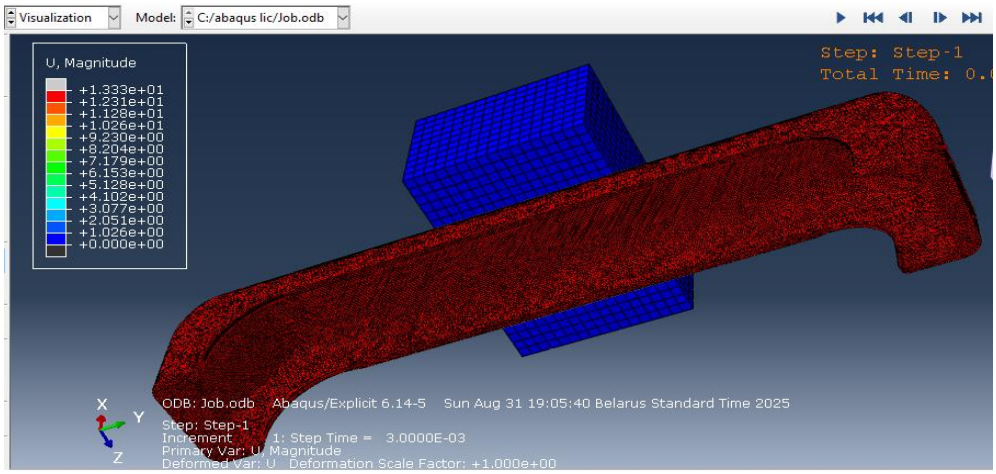

Figure 4.10 Deformation of Composite Bumper

Production Cost of the Composite bumper

Material	Cost per unit	quantity (kg)	Cost(ETB)
Epoxy	1500	4	6000
Glass	500	1	500
Sisal	200	0.5	250
Wool	100	0.3	150
Painting	-	-	1500
Labour	-	-	2800
Other	-	-	2000
Total			14000

Comparation of analyis of bumper

Charpy impact test was conducted on the glass/sisal/wool fibre composite bumper to determine its properties for the comparative analysis with the steel bumpers. Result showed that the composite bumper can absorb a maximum energy of 49.34kJ/m^2 when compared with steel bumper of 23.27KJ/m^2 the same size.

Steel bumper has the highest cost of N32,000 which is more than the costs of composite bumpers at N14,000. When compared, the Glass/sisal/wool fiber reinforced composite bumper costs decrease by 56.25% than that of the existing steel bumpers.

Weight Saving of producing the composite bumper, it was weighed on a digital scale; the weight was found to be 3.8kg, and the weight of the steel bumper was found to be 5.16kg. This means that a

weight saving of 1.36kg was achieved. This weight difference can influence the reduction of fuel consumption and increase the efficiency of the car. These factors justify the objective of the research.

Average fuel saving = $\frac{0.38\ \mathrm{L}*\mathrm{reduced\ mass}}{100\mathrm{kg}*100\mathrm{km}} = 0.0052l/100Km$

An average fuel saved 0.0052 liters per100Km was achieved by the optimized composite bumper beam of the vehicle.

5 CONCLUSION AND RECOMMENDATION

5.1 CONCLUSION

This research successfully developed a Toyota Corolla car bumper using a composite of glass, sisal, and wool fibers reinforced with epoxy resin through the hand lay-up technique. Significant quantities of sisal and wool fibers were processed as raw materials, and a rectangular mold was utilized for fabrication. The resulting high-strength, lightweight bumper demonstrated impressive mechanical properties, including a tensile strength of 114.07 MPa, an impact strength of 112.5 kJ/m² at an impact velocity of 2.22 m/s, a compressive strength of 92.2 MPa, and a flexural strength of 1270.6 MPa.

Impact analysis using Genetic Algorithm software indicated that the composite bumper exhibited lower deformation (89 mm) compared to a traditional steel bumper (134 mm), showcasing a 74.6% increase in strength. The composite material absorbed 56.7% more internal energy during impact than mild steel, resulting in minimized deflection and optimized stress distribution. Cost analysis revealed a 56.25% savings with the glass/sisal/wool composite bumper compared to existing options. Additionally, the optimized composite bumper contributed to an average fuel saving of 0.0052 liters per 100 km, highlighting its economic and environmental benefits over conventional materials.

5.2 RECOMMENDATION

It is advisable to process sisal fiber into knitted mat form to ensure uniform stress distribution during the fabrication of bumpers, which will enhance the mechanical performance and durability of the composite materials. Promoting the cultivation of sisal fiber plantations in Ethiopia is crucial for facilitating sustainable production, thereby enabling the development of local automobile industries and reducing reliance on imported materials. Continued research should focus on improving the properties and processing techniques of sisal fiber composites, with large-scale production efforts prioritized to meet the growing demand in the automotive sector. Additionally, establishing a dedicated sisal fiber processing factory in Tigray would streamline the processing of sisal fibers for both domestic use and export, contributing to the region's economic growth. Finally, further studies on the thermal effects of composite materials in automobile applications are essential, as understanding how temperature variations impact stress and performance will optimize the design and functionality of composite bumpers, leading to improved material resilience under varying environmental conditions.

6 Limitations of the study

During the study, several limitations were encountered. Firstly, the availability of high-quality sisal and wool fibers in sufficient quantities affected the consistency of the composite material properties. Additionally, challenges in the hand lay-up technique, such as ensuring uniform resin application and minimizing void content, impacted the overall quality of the fabricated samples. The chemical treatment process for the fibers required precise control of parameters like concentration and immersion time, which were sometimes difficult to maintain consistently. Moreover, equipment limitations, such as the capacity of the universal testing machine, restricted the range of mechanical tests that could be performed. Finally, time constraints limited the ability to conduct extensive long-term studies on the durability and performance of the composites under varying environmental conditions.

7 References

‘— D E C L A R A T I O N — Federal Motor Vehicle Safety , Bumper and Theft Prevention Standards’ (2022), 7(3), p. 75124.

‘1 . Classification of Composite Materials’ (2004), pp. 1–2.

‘169.73 bumpers, safeguards.’ (2009), pp. 169–170.

Achema, F. *et al.* (2017) ‘Application of Glass Fibre Reinforced Composite in the Production of Light Weight Car Bumper (A Case Study of the Mechanical Properties)’, *International Journal of Engineering Research & Technology*, 6(07), pp. 575–579.

Alajmi, A. *et al.* (2024) ‘An Experimental and Numerical Investigation into the Durability of Fibre / Polymer Composites with Synthetic and’.

Ali, A. *et al.* (no date) ‘Prediction of Mechanical , Thermal and Electrical Properties of Wool / Glass Fiber based Hybrid Composites Prediction of Mechanical , Thermal and Electrical Properties of Wool / Glass Fiber based Hybrid Composites’. Available at: https://doi.org/10.1088/1757-899X/928/2/022004.

Allafi, F. *et al.* (2022) ‘Advancements in Applications of Natural Wool Fiber : Review Advancements in Applications of Natural Wool Fiber : Review’, *Journal of Natural Fibers*, 19(2), pp. 497–512. Available at: https://doi.org/10.1080/15440478.2020.1745128.

Arruda, M.R.T., Castro, L. and Correia, J.R. (2021) ‘Composites Part C : Open Access Tsai – Wu based orthotropic damage model’, *Composites Part C: Open Access*, 4(February), p. 100122. Available at: https://doi.org/10.1016/j.jcomc.2021.100122.

Arthanarieswaran, V.P., Kumaravel, A. and Kathirselvam, M. (2014) ‘Evaluation of mechanical properties of banana and sisal fiber reinforced epoxy composites : Influence of glass fiber hybridization’, 64, pp. 194–202.

Ashik, K.P. and Sharma, R.S. (2015) ‘A Review on Mechanical Properties of Natural Fiber Reinforced Hybrid Polymer Composites’, (September), pp. 420–426.

Background, F. (2013) ‘CO’.

Bajpai, P. (no date) ‘Genetic Algorithm – an Approach to Solve Global Optimization Problems’, 1(3), pp. 199–206.

Belingardi, G. *et al.* (2015) ‘Alternative lightweight materials and component manufacturing technologies for vehicle frontal bumper beam’, *Composite Structures*, 120, pp. 483–495. Available at: https://doi.org/10.1016/j.compstruct.2014.10.007.

Betelie, A.A. *et al.* (2019) ‘Mechanical properties of sisal-epoxy composites as functions of fiber-to-epoxy ratio’, 6(October), pp. 985–996. Available at: https://doi.org/10.3934/matersci.2019.6.985.

Bichang, D.O. *et al.* (2022) ‘A Review on the Parameters Affecting the Mechanical , Physical , and Thermal Properties of Natural / Synthetic Fibre Hybrid’, 2022. Available at:

https://doi.org/10.1155/2022/7024099.

Blicblau, A.S. (2014) ‘Novel composites utilizing raw wool and polyester resin Novel composites utilizing raw wool and polyester resin’, (September 1997). Available at: https://doi.org/10.1023/A.

Buba, W.D., Bello, A.A. and Jatau, J.S. (2023) ‘Production and Performance Evaluation of Sisal Fibre (Agave Sisalana) As Composite Material for Car Bumper’, *European Journal of Mechanical Engineering Research*, 10(1), pp. 46–81. Available at: https://doi.org/10.37745/ejmer.2014/vol10n14681.

Capretti, M. *et al.* (2024) ‘Natural Fibre and Hybrid Composite Thin-Walled Structures for Automotive Crashworthiness: A Review’, *Materials*, 17(10). Available at: https://doi.org/10.3390/ma17102246.

Carr, J. (2014) ‘An Introduction to Genetic Algorithms’, pp. 1–40.

Chinnasamy, J. and Periasamy, S. (2021) ‘Design and Analysis of Bumper Beam and Energy Absorbers by Using Composite Materials Design and Analysis of Bumper Beam and Energy Absorbers’. Available at: https://doi.org/10.1088/1757-899X/1055/1/012044.

Dange, M. V, Buktar, R.B. and Raykar, N.R. (2015) ‘Design and Analysis of an Automotive Front Bumper Beam for Low-Speed Impact’, 12(2), pp. 17–27. Available at: https://doi.org/10.9790/1684-12241727.

Das, S. (2001) ‘the Cost of Automotive Polymer Composites : a Review and Assessment of Doe ’ S Lightweight’, *Oak Ridge National Laboratory*, pp. 1–47.

Dashtizadeh, Z. *et al.* (2017) ‘SCIENCE & TECHNOLOGY Mechanical and Thermal Properties of Natural Fibre Based Hybrid Composites : A Review’, 25(4), pp. 1103–1122.

Deshpande, A.M. and Brown, N. (2022) ‘TigerPrints Design and Development of a Multi-material , Cost-competitive , Lightweight Mid-size Sports Utility Vehicle ’ s Body-in-White’.

Du, B. *et al.* (2023) ‘Application of Lightweight Structure in Automobile Bumper Beam: A Review’, *Materials*, 16(3). Available at: https://doi.org/10.3390/ma16030967.

Dugvekar, M. and Dixit, S. (2021) ‘Mechanical Properties Of Glass Fibers Reinforced Composites : A Concise Review Mechanical Properties Of Glass Fibers Reinforced Composites : A Concise Review’, 12(6), pp. 915–922.

Gangil, B. *et al.* (2020) ‘Natural and Synthetic Fibers for Hybrid Composites’.

Gupta, M.K. *et al.* (2015) ‘Mechanical and Water Absorption Properties of Hybrid Sisal / Glass Fibre Reinforced Epoxy Composite’, 3(2), pp. 208–219.

Gupta, M.K. and Deep, V. (2017) ‘Effect of Stacking Sequence on Flexural and Dynamic Mechanical Properties of Hybrid Sisal / Glass Polyester Composite’, 5(1), pp. 53–62.

Gupta, M.K. and Srivastava, R.K. (2016a) ‘A Review on Characterization of Hybrid Fibre Reinforced Polymer Composite’, 4(1), pp. 1–7.

Gupta, M.K. and Srivastava, R.K. (2016b) 'Mechanical Properties of Hybrid Fibers-Reinforced Polymer Composite : A Review', 2559. Available at: https://doi.org/10.1080/03602559.2015.1098694.

Gurmu, D.N. (2023) 'Experimental Investigation on Effect of Weight Fraction of Sisal Fiber on Mechanical Properties of Sisal-E-Glass Hybrid Polymer Composites', 2023. Available at: https://doi.org/10.1155/2023/3948500.

Harris, B. (1999) 'ENGINEERING COMPOSITE MATERIALS'.

Hochard, Christian *et al.* (2017) 'Optimum design of laminated composite structures To cite this version : HAL Id : hal-00088234', 8223(03), pp. 159–165.

Huzaifa, M. *et al.* (2024) 'Exploring mechanical properties of eco-friendly hybrid epoxy composites reinforced with sisal, hemp, and glass fibers', *Journal of Materials Research and Technology*, 33(August), pp. 2785–2793. Available at: https://doi.org/10.1016/j.jmrt.2024.08.189.

Islam, T. *et al.* (2024) 'Advancements and challenges in natural fiber-reinforced hybrid composites: A comprehensive review', *SPE Polymers*, 5(4), pp. 481–506. Available at: https://doi.org/10.1002/pls2.10145.

ISO (2008) 'INTERNATIONAL STANDARD Plastics--Determination of water adsorption', *International Organization for Standardization*, 2008, pp. 1–15.

Joseph, K., Dias, R., *et al.* (1999) 'A REVIEW ON SISAL FIBER REINFORCED POLYMER', (May 2014).

Joseph, K., James, B., *et al.* (1999) 'A REVIEW ON SISAL FIBER REINFORCED POLYMER', (083), pp. 367–379.

Karatas, M.A. (2018) 'A review on machinability of carbon fi ber reinforced polymer (CFRP) and glass fi ber reinforced polymer (GFRP) composite materials', 14, pp. 318–326. Available at: https://doi.org/10.1016/j.dt.2018.02.001.

Kumar, G. (2017) 'No Title', (May).

Kumar, R. and Shelare, S. (2019) 'Different method of Fabrication of composite material-A review', *Journal of Emerging Technologies and Innovative Research*, 6(3), pp. 530–538. Available at: https://doi.org/10.6084/m9.jetir.JETIREL06080.

Marzbanrad, J., Alijanpour, M. and Kiasat, M.S. (2009) 'Design and analysis of an automotive bumper beam in low-speed frontal crashes', *Thin-Walled Structures*, 47(8–9), pp. 902–911. Available at: https://doi.org/10.1016/j.tws.2009.02.007.

Melkamu, A., Kahsay, M.B. and Tesfay, A.G. (2018) 'Mechanical and water-absorption properties of sisal fiber (Agave sisalana) -reinforced polyester composite', *Journal of Natural Fibers*, 00(00), pp. 1–9. Available at: https://doi.org/10.1080/15440478.2018.1441088.

Method, S.T. (2002) 'Standard Test Method for Tensile Properties of Polymer Matrix Composite Materials 1', 15.

Method, T. (no date) ‘Standard Test Method for Compressive Properties of Polymer Matrix Composite Materials with Unsupported Gage Section by Shear iTeh Standards iTeh Standards Document Preview’, 08, pp. 2–3.

Mohammadi, H. *et al.* (2023) ‘Lightweight Glass Fiber-Reinforced Polymer Composite for Automotive Bumper Applications: A Review’, *Polymers*, 15(1), pp. 1–30. Available at: https://doi.org/10.3390/polym15010193.

Nagavally, R.R. (2016) ‘COMPOSITE MATERIALS - HISTORY , TYPES , FABRICATION TECHNIQUES , ADVANTAGES , AND APPLICATIONS’, pp. 25–30.

Neto, J. *et al.* (2022) ‘A Review of Recent Advances in Hybrid Natural Fiber Reinforced Polymer Composites’. Available at: https://doi.org/10.32604/jrm.2022.017434.

NHTSA (2011) ‘Quick Reference Guide to Federal Motor Vehicle Safety Standards and Regulations’, *National Highway Traffic Safety Administration* [Preprint], (February).

Nijssen, R.P.L. (no date) *Composite Materials An Introduction*.

No, S. (2023) ‘Title 49 — Transportation Subtitle B — Other Regulations Relating to Transportation Chapter V — National Highway Traffic Safety Administration , Department of Transportation Part 571 — Federal Motor Vehicle Safety Standards Subpart B — Federal Motor Vehic’, 208(208), pp. 1–128.

Pellicer, E. (2021) *Smart Composite Materials: An Introduction*, *Encyclopedia of Materials: Composites*. Available at: https://doi.org/10.1016/B978-0-12-819724-0.00092-6.

‘polymers-13-03514.pdf.crdownload’ (no date).

Presentation, C. (no date) ‘Composite fabrication techniques’, pp. 1–38.

Rajak, D.K. *et al.* (no date) ‘Fiber-Reinforced Polymer Composites ’:

Ramasamy, S. *et al.* (2023) ‘Study of Various Properties of Chemically Treated Lignocellulosic Cissus quadrangularis Stem Fiber for Composite Reinforcement Study of Various Properties of Chemically Treated Lignocellulosic Cissus quadrangularis Stem Fiber for Composite Reinforcement’, *Journal of Natural Fibers*, 20(1). Available at: https://doi.org/10.1080/15440478.2022.2161689.

Ravi, P. (2023) ‘Investigation of Physical , Mechanical , Tribological and Biodegradable Properties of Hybrid Natural Fiber Reinforced Polymer Composite’.

Ravikumar, P. *et al.* (2022) ‘Evaluation of Mechanical and Water Absorption Behaviors of Jute / Carbon Fiber Reinforced Polyester Hybrid Composites Evaluation of Mechanical and Water Absorption Behaviors of Jute / Carbon Fiber Reinforced Polyester Hybrid Composites’, *Journal of Natural Fibers*, 19(13), pp. 6521–6533. Available at: https://doi.org/10.1080/15440478.2021.1924339.

Reddy, B.V.K. (no date) ‘Impact Analysis of Front Frame Car Bumper’, pp. 1400–1405.

Rosenthal, G. (2009) ‘Economic and Social Council’, *The Oxford Handbook on the United Nations*,

2020(December 2020). Available at: https://doi.org/10.1093/oxfordhb/9780199560103.003.0007.

Safety, E. and Systems, S. (2025) '§ 46 . 2-1063 . Alteration of suspension system ; bumper height limits ; raising body above frame rail', pp. 1–2.

Series, I.O.P.C. and Science, M. (no date) 'Properties of Jute and Sheep Wool Fiber Reinforced Hybrid Polypropylene Composites Properties of Jute and Sheep Wool Fiber Reinforced Hybrid Polypropylene Composites'. Available at: https://doi.org/10.1088/1757-899X/438/1/012029.

Seydibeyoğlu, M.Ö. *et al.* (2023) 'Review on Hybrid Reinforced Polymer Matrix Composites with Nanocellulose, Nanomaterials, and Other Fibers', *Polymers*, 15(4). Available at: https://doi.org/10.3390/polym15040984.

Shok, P.U.A., Abu, P.H.U.B. and Aidu, D.R.V.N.A.G.A.P.R.N. (2016) 'Design Optimization of Car Front Bumper', 08(22), pp. 4306–4311.

Sonar, T. *et al.* (2015) 'Natural Fiber Reinforced Polymer Composite Material-A Review', pp. 142–147.

Sosiati, H. and Rizky, A.M. (no date) 'Mechanical , Thermal and Morphological Properties of Sisal Fibres Mechanical , Thermal and Morphological Properties of Sisal Fibres'. Available at: https://doi.org/10.1088/1757-899X/455/1/012014.

Specimens, P. and Materi-, E.I. (2010) 'Standard Test Methods for Flexural Properties of Unreinforced and Reinforced Plastics and Electrical Insulating Materials 1', (April). Available at: https://doi.org/10.1520/D0790-10.

Sticklen, J. *et al.* (1992) 'Fabricating composite materials--A comprehensive problem-solving architecture based on generic tasks', *IEEE Expert*, 7(2), pp. 43–53. Available at: https://doi.org/10.1109/64.129282.

Thirumalaisamy, R. *et al.* (2023) 'Review Article Study on Water Absorption Characteristics , Various Chemical Treatments , and Applications of Biological Fiber-Reinforced Polymer Matrix Composites', 2023. Available at: https://doi.org/10.1155/2023/9903119.

Zhang, W. and Xu, J. (2022) 'Materials & Design Advanced lightweight materials for Automobiles : A review', *Materials & Design*, 221, p. 110994. Available at: https://doi.org/10.1016/j.matdes.2022.110994.

Zoccola, M. and Anceschi, A. (2024) 'Exploring the Potential Applications of Wool Fibers in Composite Materials : A Review'.

APPENDIX-A

- Rule of mixture

Total mass of composite = mass of fiber + mass of matrix $= W_C = W_F + W_M$

$$Fiber\ mass\ fraction = \frac{weight\ of\ fiber}{total\ weight} = W_{fF} = \frac{W_F}{W_F + W_M}$$

$$\text{Matrix mass fraction} = \frac{\text{mass of matrix}}{\text{total mass}} = W_{fM} = \frac{W_M}{W_F + W_M}$$

$$M_F + M_M = 1$$

ii. Fiber and matrix volume fraction (V_F, V_M) $= V_C = V_F + V_M$

$$\text{The volume of fiber} = \frac{\text{weight of fiber}}{\text{density of fiber}}$$

$$V_{fF} = \frac{V_F}{V_F + V_M} = \frac{W_F \times \rho_M}{W_F \times \rho_M + W_M \times \rho_F}$$

$$\text{Matrix volume fraction} = \frac{\text{weight of matrix}}{\text{density of matrix}}$$

$$V_{fM} = \frac{V_M}{V_F + V_M} = \frac{W_M \times \rho_F}{W \times \rho_M + W_M \times \rho_F}$$

$$V_F + V_M = 1$$

Weight and weight fraction of composite

No. laminates	weight of fiber(g)			weight fraction of fiber(%)			weight of matrix (g)	weight of composite (g)	weight fraction of matrix(%)
	G	S	W	G	S	W	E	W_C	E
GSWSG	47.8	23.2	8.1	8.25	4	1.4	500	579.1	86.35
SGWGS	47.8	23.2	8.1	8.25	4	1.4	500	579.1	86.35
WWWWW	-	-	40.1	-	-	7.5	500	540.1	92.5
SSSSS	-	69.6	-	-	12.2	-	500	569.6	87.8
GGGGG	143.4	-	-	22.3	-	-	500	643.4	77.7

Volume and volume fraction of composite

No. Laminates	Volume of fiber (cm^3)			Volume of matrix (cm^3)	Volume fraction of fiber(%)			Total volume fraction of fiber and matrix (%)		Total Volume of composite (cm^3)
	G	S	W	E	G	S	W	V_{FF}	V_{FM}	V_C
GSWSG	18.8	16.4	6.23	384.6	18	18	9	45	55	426.03
SGWGS	18.8	16.4	6.23	384.6	18	18	9	45	55	426.03
WWWWW	-	-	6.23	384.6	-	-	45	45	55	390.83
SSSSS	-	16.4	-	384.6	-	45	-	45	55	401
GGGGG	18.8	-	-	384.6	45	-	-	45	55	403.4

Theoretical and actual density of composite

Sample	Theoretical density=Wc/Vc(g/cm^3)	Actual density or measured(g/cm^3)
GSWSG	1.359	1.348
SGWGS	1.359	1.33
WWWWW	1.382	1.26
SSSSS	1.42	1.18
GGGGG	1.595	1.41

Theoretical density, $\rho_C = \frac{W_C}{V_C} = \frac{W_F + W_M}{W_F \times \rho_M + W_M \times \rho_F}$

APPENDIX -B

- Experimental result and Material property of composite

Sample	Strength					Water absorption (%)	Density g/cm^3	
	Tensile (Mpa)	Ultimate tensile (Mpa)	Compressive (Mpa)	Impact (KJ/m^2)	Flexural (Mpa)		Theoretical	Actual
GSWSG	114.07	145.92	181.83	112.5	1270.6	3	1.359	1.341
SGWGS	85.8	105.86	118.56	87.5	704.1	9	1.359	1.33
WWWWW	105.4	127.27	107.65	50	1753.1	4	1.382	1.26
SSSSS	102.5	145.38	126.66	80	1284	11	1.42	1.18

Water absorption (%)

Laminates	Water absorption (%)

	24hr	72hr	120hr	168hr	216hr	264hr	312hr	360hr
GSWSG	0.2	0.5	0.8	1.2	1.4	1.6	3	3
SGWGS	1	3	4	6	8	9	8	9
WWWWW	0.2	0.6	1.5	2	3	3.75	4	4
SSSSS	4	6	8	9	9.5	10	11	11

$$\%\ water\ absorption = \frac{W_f - W_i}{W_i} \times 100$$

Material property of bumper beam composite

Moduli parameters	Symbol	Glass/epoxy	Sisal/epoxy	Wool/epoxy
Volume ratio	V_f	0.18	0.18	0.09
Density	ρ (g/cm3)	1.5 2	0.967	0.832
Longitudinal modulus	E_1 (MPa)	16370	5930	3680
Transversal modulus	E_2 (MPa)	3480	3070	2950
Shear modulus	G_{12} (MPa)	1410	1240	1140
Longitudinal tensile strain	e_L(mm)	2	1.95	3.4
Poissons ratio	μ_{12}	0.34	0.345	0.354
Longitudinal tension	X_t (MPa)	499.2	148.2	60
Longitudinal compression	X_c (MPa)	327.4	138.4	68.65
Transverse tension	Y_t (MPa)	68	59	49.1
Transverse compression	Y_c (MPa)	46.7	41.3	34.55
Shear strength	τ_{12} (MPa)	35.4	28.38	29.58

APPENDIX-C

Classical laminate theory

- Ply orrentation theta = [90,15,0,15,90]
- Transform stiffness matrix(Qbar)

$$\begin{bmatrix} \bar{Q}_{11} & \bar{Q}_{12} & \bar{Q}_{16} \\ \bar{Q}_{12} & \bar{Q}_{22} & \bar{Q}_{26} \\ \bar{Q}_{16} & \bar{Q}_{26} & \bar{Q}_{66} \end{bmatrix}$$ =1.0e+09 *[3.2716 1.1287 0; 1.1287 6.3194 0; 0 0 1.2400]

- Extention stiffness matrix [A]= $A_{ij} = \sum_{k=1}^{n} \left[\bar{Q}_{ij}\right]_k (h_k - h_{k-1})$

[3.3047e+08,4.636e+07,0;4.636e+07,2.714e+08,0;0,0,5.237e+07]

- Bending stiffness matrix [D]= $D_{ij} = \frac{1}{3}\sum_{k=1}^{n}\left[\bar{Q}_{ij}\right]_k (h^3{}_k - h^3{}_{k-1})$

[4.099e+03,5.7506e+02,0;5.7506e+02,3.367e+03,0;0,0,6.4958e+02]

- Global_stress of composite

$$\begin{bmatrix}\sigma_x\\ \sigma_y\\ \tau_{xy}\end{bmatrix} = \begin{bmatrix}\bar{Q}_{11} & \bar{Q}_{12} & \bar{Q}_{16}\\ \bar{Q}_{12} & \bar{Q}_{22} & \bar{Q}_{26}\\ \bar{Q}_{16} & \bar{Q}_{26} & \bar{Q}_{66}\end{bmatrix}_k \begin{bmatrix}\varepsilon_x\\ \varepsilon_y\\ \gamma_{xy}\end{bmatrix} =$$ 1.0e+07 *[2.1640; -2.1956; 0]pa

- Mid plane strain(e0)

$$\begin{bmatrix}\varepsilon^0{}_x\\ \varepsilon^0{}_y\\ \gamma^0{}_{xy}\end{bmatrix} = \begin{bmatrix}A^*{}_{11} & A^*{}_{12} & A^*{}_{16}\\ A^*{}_{12} & A^*{}_{22} & A^*{}_{26}\\ A^*{}_{16} & A^*{}_{26} & A^*{}_{66}\end{bmatrix}\begin{bmatrix}N_x\\ N_y\\ N_{xy}\end{bmatrix}$$=[0.0045; -0.0045; 0]

- Mid plane curvature(K)

$$\begin{bmatrix}K_X\\ K_Y\\ K_{XY}\end{bmatrix} = \begin{bmatrix}D^*{}_{11} & D^*{}_{12} & D^*{}_{16}\\ D^*{}_{12} & D^*{}_{22} & D^*{}_{26}\\ D^*{}_{16} & D^*{}_{26} & D^*{}_{66}\end{bmatrix}\begin{bmatrix}M_x\\ M_y\\ M_{xy}\end{bmatrix}$$ =[1.28; -0.158; 0]m

- K[th] layer strain laminate composite(epsilonk)

$$\begin{bmatrix}\varepsilon_x\\ \varepsilon_y\\ \gamma_{xy}\end{bmatrix}^k = \begin{bmatrix}\varepsilon^0{}_x\\ \varepsilon^0{}_y\\ \gamma^0{}_{xy}\end{bmatrix} + Z\begin{bmatrix}\varepsilon_x\\ \varepsilon_y\\ \gamma_{xy}\end{bmatrix}$$ =[0.0038 ; -0.0005 ; 0]

- Global strain(epsilon)

$$\begin{bmatrix}\varepsilon_x\\ \varepsilon_y\\ \gamma_{xy}\end{bmatrix} = \begin{bmatrix}\varepsilon^0{}_x\\ \varepsilon^0{}_y\\ \gamma^0{}_{xy}\end{bmatrix} + Z\begin{bmatrix}K_x\\ K_y\\ K_{xy}\end{bmatrix}$$ = [0.0083 ; -0.0050 ; 0]

- The optimized max_sress

1.3073+07 pa

- Maximum optimize mass(mbest)

2.5030 Kg

- Optimized thickness of composite bumper beam(tbest)of glass, sisal and wool fiber

[0.0012,0.0012,7.0e-04]m or tatal thickness optimized is 5.5mm or 0.0055m

- Ply thickness of composite bumper beam(Z)

[0.0012,0.0012,3.5e-04]

- Applid load and bending moment of composite bumper

M= [80.36;0;0]Nm

N= [27.572; 0; 0]KN

- Global stress for each lamina

$$\begin{bmatrix}\sigma_x\\ \sigma_y\\ \tau_{xy}\end{bmatrix}=\begin{bmatrix}\bar{Q}_{11} & \bar{Q}_{12} & \bar{Q}_{16}\\ \bar{Q}_{12} & \bar{Q}_{22} & \bar{Q}_{26}\\ \bar{Q}_{16} & \bar{Q}_{26} & \bar{Q}_{66}\end{bmatrix}_k\begin{bmatrix}\varepsilon_x\\ \varepsilon_y\\ \gamma_{xy}\end{bmatrix}$$

- Global stress of Glass/epoxy(pa)

Q11_G=1.678e+10, Q12_G=1.213e+09, Q22_G=3.567e+09, Q66_G=1.41e+09

$\sigma_x = 133.2Mpa, \sigma_y = -7.8Mpa, \tau_{12} = 0, \tau_{xy} = 0$

- Global stress Sisal/epoxy

Q11_S= 6.319e+09, Q12_S= 1.128e+09, Q22_S= 3.271e+09, Q66_S= 1.24e+09

$\sigma_x = 46.8Mpa, \sigma_y = -6.97Mpa, \tau_{xy} = 0$

- Wool/epoxy

Q11_W= 4.09e+09, Q12_W= 1.161e+09, Q22_W= 3.279e+09 , Q66_W= 1.14e+09

$\sigma_x = 28.14Mpa, \sigma_y = -6.7Mpa, \tau_{xy} = 0$

- Local stress

$$\begin{bmatrix}\sigma_1\\ \sigma_2\\ \tau_{12}\end{bmatrix}=[T]\begin{Bmatrix}\sigma_X\\ \sigma_Y\\ \tau_{XY}\end{Bmatrix}, [T]=\begin{bmatrix}C^2 & S^2 & 2CS\\ S^2 & C^2 & -2CS\\ -SC & SC & C^2-S^2\end{bmatrix}$$

- Local stress of Glass/Epoxy

$\sigma_1 = 133.2Mpa, \sigma_2 = -7.8Mpa, \tau_{12} = 0$

- Local stress of Sisal/Epoxy

$\sigma_1 = 46.8Mpa, \sigma_2 = -6.97Mpa, \tau_{12} = 0$

- Local stress of Wool/Epoxy

$\sigma_1 = 28.14Mpa, \sigma_2 = -6.7Mpa, \tau_{12} = 0$

- Strength ratio (Tsai wu)

SR.>1, =7.069

APPENDIX _D

```
% Main script BY-MULU GIDEY

% Number of variables (tg, ts, tw)
nvars = 3;

% Lower and upper bounds for ply thickness
LB = [0.0012, 0.0012, 0.0007]; % Lower bounds for ply thickness of Glass, Sisal,
Wool
UB = [0.0015, 0.0015, 0.001]; % Upper bounds for ply thickness of Glass, Sisal,
Wool

% GA options
options = optimoptions('ga', ...
    'PopulationSize', 100, ...
    'MaxGenerations', 200, ...
    'EliteCount', 2, ...
    'MutationFcn', {@mutationadaptfeasible}, ...
    'CrossoverFraction', 0.8, ...
    'FunctionTolerance', 1e-9, ...
    'ConstraintTolerance', 1e-4, ...
    'PlotFcn', @gaplotbestf);

% Run the GA solver
[tbest, mbest] = ga(@(x) myfitness(x), nvars, [], [], [], [], LB, UB, @(x)
Tsai_wu_total_constraint(x), options);

% Display results
disp('Optimized Thicknesses (tg, ts, and tw):');
disp(tbest);
disp('Best Fitness Value (Mass):');
disp(mbest);
% Compute and Display Maximum Stress at Optimized Thicknesses
[~, max_stress] = compute_Tsai_wu_total([tbest(1), tbest(2), tbest(3), tbest(2),
tbest(1)], [90, 15, 0, 15, 90]);
disp('Maximum Stress Value at Optimized Thicknesses (Pa):');
disp(max_stress);

% Define objective function
function mass = myfitness(x)
    tg = x(1); % Thickness of glass fiber
    ts = x(2); % Thickness of sisal fiber
    tw = x(3); % Thickness of sheep wool fiber

    % Constants
    Lt = 2.055; % Total length of bumper in meters
    Le = 1.44;  % Effective length of bumper in meters
    B = 0.152;  % Effective breadth of bumper in meters
```

```
    D = 0.055; % Effective dePth of bumper in meters
    dens_glass = 1.52e3; % Density of glass in kg/m^3
    dens_sisal = 1.27e3; % Density of sisal in kg/m^3
    dens_wool = 1.3e3;   % Density of wool in kg/m^3
    vehicle_mass = 1242; % kg
    velocity = 2.222; % m/s
    N = 5; % Number of layers

    % Total ply thickness
    ply_thickness = (2 * tg + 2 * ts + tw);
    tensile_strength = 114.07e6; % Pa

    % Mass calculation
    mass =((Lt * B)+(2*B * D))* (2 * tg * dens_glass + 2 * ts * dens_sisal + tw *
dens_wool);

    % Kinetic Energy (J)
    KE = 0.5 * vehicle_mass * velocity^2;
end

% Define constraint function
function [c, ceq] = Tsai_wu_total_constraint(x)
    tg = x(1); % Thickness of glass fiber
    ts = x(2); % Thickness of sisal fiber
    tw = x(3); % Thickness of sheep wool fiber

    % Constants reused from myfitness
    N = 5; % Number of layers
    ply_thickness = (2 * tg + 2 * ts + tw); % Total ply thickness
    tensile_strength = 114.07e6; % Pa

    % Kinetic Energy calculation
    vehicle_mass = 1242; % kg
    dens_glass = 1.52e3; % Density of glass in kg/m^3
    dens_sisal = 1.27e3; % Density of sisal in kg/m^3
    dens_wool = 1.3e3;   % Density of wool in kg/m^3
    KE = 0.5 * vehicle_mass * (2.222^2); % using the velocity defined in
myfitness

    % Constraints
    c(1) = KE - (0.5 * N * ply_thickness * tensile_strength); % Energy absorption
constraint
    c(2) = (N * ply_thickness * (dens_glass + dens_sisal + dens_wool) * 2.055 *
0.152 / vehicle_mass) - tensile_strength; % Stress constraint
    ceq = []; % No equality constraints
end

% Tsai-Wu Computation
function [Tsai_wu_total, max_stress] = compute_Tsai_wu_total(thicknesses, theta)
    % Load conditions
    N = [27.572e3;0; 0]; % Normal force of bumper beam(N)
    M = [80.36; 0; 0]; % Bending moments of bumper beam(Nm)
    R= 2;% Marginal safety

    % Material properties for glass, sisal, and wool
```

```
    % Glass_epoxy(plies 1 and 5)
    E1_G = 16.37e9;  % Longitudinal modulus (Pa)
    E2_G = 3.48e9;
    V12_G = 0.34;
    G12_G = 1.41e9;
    Xt_G = 499.2e6;
    Xc_G = 327.4e6;
    Yt_G = 68e6;
    Yc_G = 46.7e6;
    Sxy_G = 35.4e6;

    % Sisal_epoxy(plies 2 and 4)
    E1_S = 5.93e9;
    E2_S = 3.07e9;
    V12_S = 0.345;
    G12_S = 1.24e9;
    Xt_S = 148.2e6;
    Xc_S = 138.4e6;
    Yt_S = 59e6;
    Yc_S = 41.3e6;
    Sxy_S = 28.38e6;

    % Wool_epoxy(ply 3)
    E1_W = 3.68e9;
    E2_W = 2.95e9;
    V12_W = 0.354;
    G12_W = 1.14e9;
    Xt_W = 60e6;
    Xc_W = 68.65e6;
    Yt_W = 49.1e6;
    Yc_W = 34.55e6;
    Sxy_W = 29.58e6;

    % Initialize matrices
    D11 = 0; D12 = 0; D22 = 0; D66 = 0;
    A11 = 0; A12 = 0; A22 = 0; A66 = 0;

    % Number of layers
    theta = [90, 15, 0, 15, 90 ]; % ply orientations
    thicknesses = [thicknesses(1), thicknesses(2), thicknesses(3),
thicknesses(2), thicknesses(1)];

    % Calculate properties and stiffness matrices
    z_current = -sum(thicknesses)/2; % Start at the bottom of the laminate
    for i = 1:length(thicknesses)
        t = thicknesses(i);
        z_bottom = z_current;
        z_top = z_bottom + t;
        z_current = z_top;
        theta_deg = theta(i) * pi / 180;
        c = cos(theta_deg);
        s = sin(theta_deg);

        % Material selection logic...
        if mod(i, 3) == 1 % Glass
            Q11 = E1_G / (1 - V12_G * (V12_G * E2_G / E1_G));
```

```
            Q12 = V12_G * E2_G / (1 - V12_G * (V12_G * E2_G / E1_G));
            Q22 = E2_G / (1 - V12_G * (V12_G * E2_G / E1_G));
            Q66 = G12_G;
        elseif mod(i, 3) == 2 % Sisal
            Q11 = E1_S / (1 - V12_S * (V12_S * E2_S / E1_S));
            Q12 = V12_S * E2_S / (1 - V12_S * (V12_S * E2_S / E1_S));
            Q22 = E2_S / (1 - V12_S * (V12_S * E2_S / E1_S));
            Q66 = G12_S;
        else % Wool
            Q11 = E1_W / (1 - V12_W * (V12_W * E2_W / E1_W));
            Q12 = V12_W * E2_W / (1 - V12_W * (V12_W * E2_W / E1_W));
            Q22 = E2_W / (1 - V12_W * (V12_W * E2_W / E1_W));
            Q66 = G12_W;
        end

        % Transform stiffness matrix
      Qbar11 = (Q11 * c^4) + (2 * (Q12 + 2 * Q66) * (c^2) * (s^2)) + (Q22 * s^4);
      Qbar12 = ((Q11 + Q22 - 4 * Q66) * (c^2) * (s^2)) + (Q12 * (c^4 + s^4));
      Qbar22 = (Q11 * s^4) + (2 * (c^2) * (s^2) * (Q12 + 2 * Q66)) + (Q22 * c^4);
      Qbar66 = (Q11 + Q22 - 2 * Q12) * (c^2) * (s^2) + (Q66 * ((c^2) - (s^2))^2);
      Qbar = [Qbar11 Qbar12 0; Qbar12 Qbar22 0; 0 0 Qbar66];

        % Update bending and extension matrices
        D11 = D11 + Qbar11 * (z_top^3 - z_bottom^3) / 3;
        D12 = D12 + Qbar12 * (z_top^3 - z_bottom^3) / 3;
        D22 = D22 + Qbar22 * (z_top^3 - z_bottom^3) / 3;
        D66 = D66 + Qbar66 * (z_top^3 - z_bottom^3) / 3;
        A11 = A11 + Qbar11 * (z_top - z_bottom);
        A12 = A12 + Qbar12 * (z_top - z_bottom);
        A22 = A22 + Qbar12 * (z_top - z_bottom);
        A66 = A66 + Qbar22 * (z_top - z_bottom);
    end

    % Extension and bending stiffness matrix
    A = [A11 A12 0; A12 A22 0; 0 0 A66];
    D = [D11 D12 0; D12 D22 0; 0 0 D66];

    % Calculate strains and curvatures
    e0 = A \ N; % Strain due to applied normal force
    K = D \ M; % Curvature due to applied bending moments

  % Initialize maximum stress
    max_stress = 0;
    zvalues = [(2*thicknesses(1)+2*thicknesses(2)+thicknesses(3))/2,
thicknesses(1)/2];  % z for upper and lower surfaces of the ply
    for j = 1:length(zvalues)
        z = zvalues(j);
        epsilonk = z * K;
        epsilone = e0 + epsilonk;
        global_stress = Qbar * epsilone;
        max_stress = max(max_stress, global_stress);

    end

    % Stress transformation matrix
```

```
    T_sg = [c^2, s^2, 2*s*c; s^2, c^2, -2*s*c; -s*c, s*c, c^2 - s^2];
    T_ss = [c^2, s^2, 2*s*c; s^2, c^2, -2*s*c; -s*c, s*c, c^2 - s^2];
    T_sw = [c^2, s^2, 2*s*c; s^2, c^2, -2*s*c; -s*c, s*c, c^2 - s^2];

    % Transform global stresses to local stresses
    local_stressg = T_sg * global_stress;
    local_stresss = T_ss * global_stress;
    local_stressw = T_sw * global_stress;

    % Local stress calculations
    sigma_1g = local_stressg(1);
    sigma_2g = local_stressg(2);
    tau_12g = local_stressg(3);

    sigma_1s = local_stresss(1);
    sigma_2s = local_stresss(2);
    tau_12s = local_stresss(3);

    sigma_1w = local_stressw(1);
    sigma_2w = local_stressw(2);
    tau_12w = local_stressw(3);

    % Tsai-Wu failure criterion (simplified version)
     F1g = 1 / Xt_G + 1 / Xc_G;
     F2g = 1 / Yt_G + 1 / Xc_G;
     F11g =(-1/(Xt_G*Xc_G));
     F12g = -0.5 * sqrt((1 / Xt_G + 1 / Xc_G) * (1 / Yt_G + 1 / Xc_G));
     F22g = 1 / (Yt_G * Yc_G);
     F66g = 1 / Sxy_G^2;
     F1s = 1 / Xt_S + 1 / Xc_S;
     F2s = 1 / Yt_S + 1 / Xc_S;
     F11s =(-1/(Xt_S*Xc_S));
     F12s = 0.5 * sqrt((1 / Xt_S + 1 / Xc_S) * (1 / Yt_S + 1 / Xc_S));
     F22s = 1 / (Yt_S * Yc_S);
     F66s = 1 / Sxy_S^2;
     F1w = 1 / Xt_W + 1 / Xc_W;
     F2w = 1 / Yt_W + 1 / Xc_W;
     F11w =(-1/(Xt_W*Xc_W));
     F12w = 0.5 * sqrt((1 / Xt_W + 1 / Xc_W) * (1 / Yt_W + 1 / Xc_W));
     F22w = 1 / (Yt_W * Yc_W);
     F66w = 1 / Sxy_W^2;
     Twg  = F1g * sigma_1g + F2g * sigma_2g + F11g * sigma_1g^2 + F22g *
sigma_2g^2 + 2 * F12g * sigma_1g * sigma_2g + F66g * tau_12g^2;
     Tws  = F1s * sigma_1s + F2s * sigma_2s + F11s * sigma_1s^2 + F22s *
sigma_2s^2 + 2 * F12s * sigma_1s * sigma_2s + F66s * tau_12s^2;
     Tww  = F1w * sigma_1w + F2w * sigma_2w + F11w * sigma_1w^2 + F22w *
sigma_2w^2 + 2 * F12w * sigma_1w * sigma_2w + F66w * tau_12w^2;

    Tsai_wu_total = (2 * Twg + 2 * Tws + Tww)==R;

end
```